AD-A042 316 AERONAUTICAL RESEARCH INST OF SWEDEN STOCKHOLM F/G 20/4
FLOW DISTURBANCES ASSOCIATED WITH PRESTON TUBES IN TURBULENT BO--ETC(U)
JAN 77 A BERTELRUD

UNCLASSIFIED FFA-127 NL

1 OF 1
ADA042316

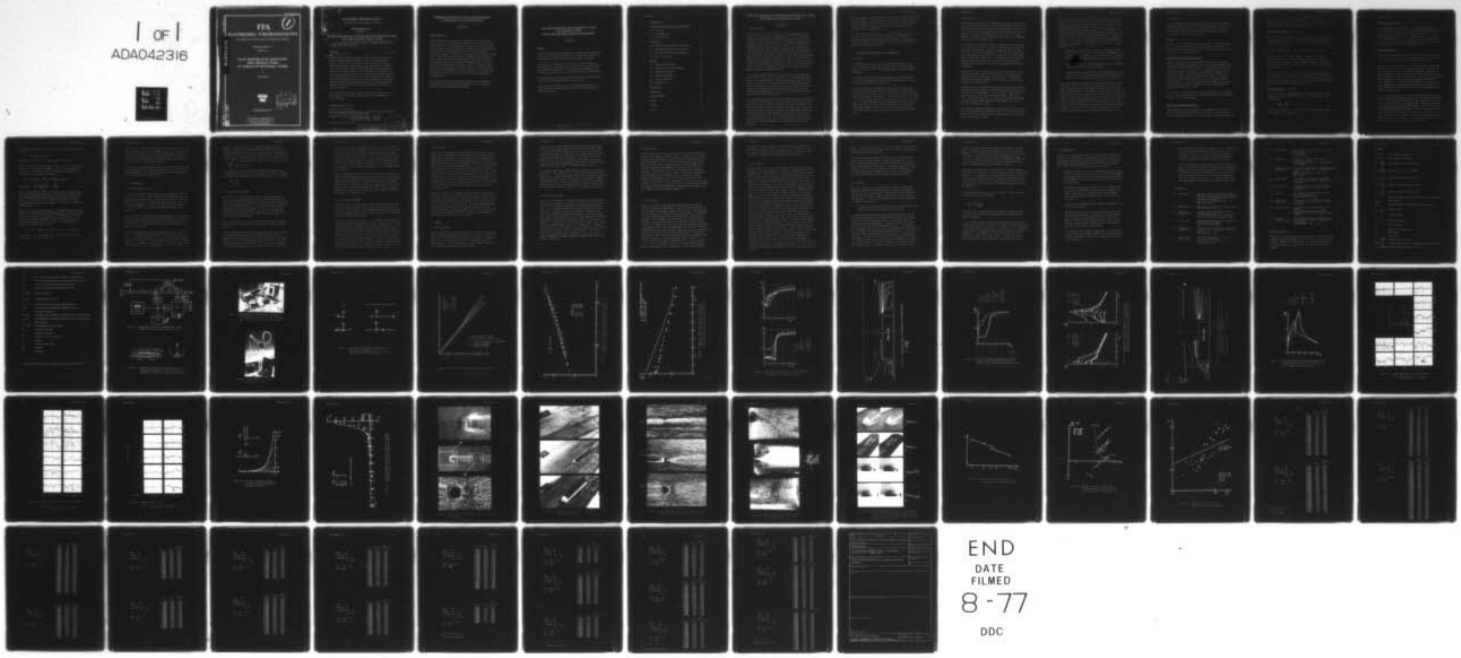

END
DATE FILMED
8-77
DDC

FFA REPORT 127

FFA

FLYGTEKNISKA FÖRSÖKSANSTALTEN

THE AERONAUTICAL RESEARCH INSTITUTE OF SWEDEN

MEDDELANDE 127

REPORT 127

FLOW DISTURBANCES ASSOCIATED WITH PRESTON TUBES IN TURBULENT BOUNDARY LAYERS

BY

Arild Bertelrud

STOCKHOLM 1977

FLYGTEKNISKA FÖRSÖKSANSTALTEN

THE AERONAUTICAL RESEARCH INSTITUTE OF SWEDEN

MEDDELANDE 127

REPORT 127

(14) FFA-127

FLOW DISTURBANCES ASSOCIATED WITH PRESTON TUBES IN TURBULENT BOUNDARY LAYERS

(Stromungsstorungen von Prestonrohren in Turbulenten Grenzschichten) (Des Perturbations des Courants a Cause des Preston Tubes dans des Couches Limites Turbulentes),

(10) ARild/Bertelrud

(11) Jan 77

(12) 63p.

SUMMARY

An investigation has been made concerning the disturbances from a surface cylinder aligned with the flow in turbulent boundary layers. The object is to study the flow around Preston tubes. Mean velocities and rms-values of the fluctuations were obtained in the centre plane of the cylinder when immersed in turbulent pipe flow. A rough estimate of the drag due to the surface cylinder was also obtained in this case. The pressure distribution near the cylinder was measured in a flat plate boundary layer, and flow visualizations were made with the oil flow technique. In addition, smoke pictures were obtained of the flow for the cases when the boundary layer thickness on the plate was negligible compared to the tube diameter.

The present results are of interest in connection with the use of Preston tubes, in particular with regard to the measurement of static pressure.

Stockholm, January 1977

This investigation was sponsored by the Defence Materiel Administration (of Sweden) Air Materiel Department.

(Contract No: FMV-F:K 82223-73-009-07-001, 74-02-26
82223-74-001-07-001, 74-08-09
82223-75-007-07-001, 75-09-12

FFA project No. AU-1133:1)

STRÖMUNGSSTÖRUNGEN VON PRESTONROHREN IN TURBULENTEN GRENZSCHICHTEN

von

Arild Bertelrud

ZUSAMMENFASSUNG

Eine Untersuchung betreffs der Störungen von einem Oberflächenzylinder, der mit der Strömung in turbulenten Grenzschichten eine Linie bildet, ist ausgeführt worden. Der Zweck war, die Strömung um Prestonrohre herum zu studieren. Durchschnittsgeschwindigkeiten und rms-Werte der Schwankungen wurden in der Mittelebene des Zylinders erhalten, wenn dieser in turbulenter Rohrströmung versenkt war. In diesem Falle wurde auch ein ungefährer Ueberschlag des Widerstandes, von dem Oberflächenzylinder verursacht, erhalten. Die Druckverteilung in der Nähe des Zylinders wurde in der Grenzschicht einer ebenen Platte gemessen, und die Strömungen wurden mit Hilfe der Ölstromtechnik sichtbar gemacht. Ausserdem wurden Rauchbilder der Strömung in den Fällen erhalten, wo die Dicke der Grenzschicht an der Platte im Vergleich mit dem Rohrdurchmesser unbedeutend war.

Die gegenwärtigen Ergebnisse haben Interesse in Verbindung mit der Anwendung von Prestonrohren, besonders wenn es sich darum handelt, den statischen Druck zu messen.

DES PERTURBATIONS DES COURANTS A CAUSE DES PRESTON TUBES DANS DES COUCHES LIMITES TURBULENTES

par

Arild Bertelrud

RÉSUMÉ

On a fait une analyse expérimentale concernant des perturbations causées par un cylindre aligné dans la direction du courant et attaché sur une surface dans une couche limite turbulente.

Le but de cette recherche est d'étudier le courant autour des tubes Preston. Des valeurs de la vitesse ont été obtenues dans le plan moyen du cylindre. Une estimation approximative de la résistance causée par la presence du cylindre a été obtenue aussi.

La distribution de la pression autour du cylindre a été mesurée dans une couche limite turbulente sur un plan.

Les résultats présentés ici, sont intéressants pour l'usage des tubes Preston, particulièrement quand il s'agit de mesurer la pression statique.

Printed at FFA Printing Office, Bromma, Sweden
ISSN: SW 0081-5640

CONTENTS

FLOW DISTURBANCES ASSOCIATED WITH PRESTON TUBES IN TURBULENT BOUNDARY LAYERS

by

Arild Bertelrud

1. INTRODUCTION

The present report is part of a project on measurement of local skin friction, currently in progress at FFA. In a recent report on calibration of Preston tubes with discussions of accuracy and alternative calibration parameters [1], a number of questions concerning the flow around the obstacles arose. In a Preston tube calibration the pressure reading is taken without modification; all disturbances to the flow created by the probe are contained in the calibration. The report referred to above indicates, however, that the results obtained are sensitive to how the static pressure is measured, and this raises the question of where the static holes should be located relative to the tube. Another subject of interest is the limiting diameter of the Preston tube. It is often argued that the reading is valid only as long as the tube does not protrude beyond the logarithmic region.

Several investigations have been made of the so called "displacement" effect of pitot tubes in shear flows [2-4], which manifests itself as an outward shift of the mean streamlines near the tube mouth. The effect of inlet geometry on yaw characteristics have also been studied [5]. Some indications of the effects on overall boundary layer parameters have been given, but to the author's knowledge no measurements of the actual flow perturbations around surface pitot tubes have been made.

In the preceding tests [1] most of the Preston tubes had the shape of right circular cylinders. The local flow near the mouth is not much affected by the internal flow and such a tube can be treated as a closed body in order to reproduce the flow field. The present investigation will attempt to determine the flow field around such an equivalent closed body immersed in a turbulent boundary layer. It is of interest to know the flow disturbances both in terms of the mean and fluctuating values, as both determine the flow conditions in a turbulent boundary layer and hence the Preston tube read out.

One may assume that the disturbances to mean and fluctuating streamwise velocities, U and u', are largest in the vertical centreplane of the cylinder. For this reason and in order to keep the effort within reasonable limits all velocity profile measurements were performed in this centreplane.

A single hot wire probe was used. Neither the transverse directional velocity changes nor the flow direction in the measurement plane could then be determined near the cylinder. The measurements should nevertheless give a picture of the flow field relative to undisturbed boundary layer flow.

2. EXPERIMENTAL APPARATUS AND DATA REDUCTION

2.1 Test pipe

The experimental rig (see Figure 1) is described in more detail in [1], where it is shown that the flow can be considered fully developed turbulent at the measurement station used in the present experiments.

It should be noted that for the experiments at low Reynolds numbers, in the laminar flow regime, the flow cannot be treated as a fully developed laminar pipe flow [6].

The test pipe has a total length of 9.35 metres, and has been assembled from lengths of plastic material (PVC) tubing, with an inner diameter of 105 mm. There is only one joint, so as to minimize the variation in flow quality. A flow straightener and a screen have been positioned between the inlet and the upstream end of the pipe. The flow through the pipe is established by connecting the downstream end of the pipe to the vacuum system of FFA's supersonic wind tunnels. Velocity control is effected by means of a valve which can be kept at any position between closed and fully open.

2.2 *Instrumentation*

The measurement rig and test configuration are shown schematically in Figures 1 and 2. Figures 3 and 4 show photographs of the instrumentation used. The static pressure was measured at Stations 9 to 13, as those values were needed for the data reduction. The static pressure at Station 1 behind the screen was used as reference pressure to improve the attainable accuracy. Details of manometer corrections etc. are found in [1].

At Station 12 a total pressure probe, denoted Rake B, consisting of 13 tubes was used [1]. For the present experiments mainly the centreline tube was used in the data reduction while the others were used to verify flow symmetry etc. The hot wire measurements were performed near Station 9 with a DISA Type 55 hot wire anemometer, fitted with a single wire. The anemometer was temperature compensating and was used with a linearizer. The signal was recorded on paper trace, but could also be monitored directly on a voltmeter.

The rms value of the fluctuating signal was recorded by a Brüel & Kjær Level Recorder Type 2305. The signal was monitored and recorded by means of an oscilloscope to see if it changed in character with Reynolds number or with proximity to the surface cylinder or the pipe wall.

Calibration of the hot wire was performed by measuring the centreline velocity in the empty test section with Rake B at Station 12, the test section being empty. The hot wire was traversed to the pipe centre at Station 9 and the reading taken. From earlier tests [1] the mean velocities at these two points have been found to agree with each other within the experimental accuracy of the total pressure tube rakes.

The surface cylinder was mounted at the bottom of the pipe and the hot wire probe was inserted through a hole in the top of the pipe. The hot wire was traversed from the upper wall down to the lower wall or the surface cylinder.

The surface cylinders used in the present experiments had external diameters of 19, 10 and 5 mm. The measurements concern the flow around a cylinder of length 127.5 mm and outer diameter 19 mm and a few comparisons with cylinders of smaller diameters were also performed. By using cylinders of different lengths mounted in different holes through the wall and locating the hot wire at different holes in the hatch, it was possible to measure the flow properties at various stations along the cylinder with a minimum of damage to the test pipe. The arguments used in support of performing the experiments in this manner with cylinders of varying diameter were:

- Measurements ahead of the cylinder are independent of its length. This is reasonable since one of the findings in [1] was that the corresponding Preston tube reading is independent of relative length for the cylinders considered here.

- Measurements over the cylinder depend only on the distance from the upstream tip of the cylinder.

- Measurements behind the cylinder appear independent of the cylinder length and dependent only on the distance from its base. This also seems to be justified by the results of [1].

The measurements were performed by mounting the hot wire probe on a manually manoeuvred traversing gear (Mitutoyo 192-101). The probe was shielded by a cover and was traversed down until the cover touched the wall. Considerable care was taken to ensure that the motion was radial and that the probe hit the wall in the centre plane. This was taken as the zero of the traversing gear and the probe was then traversed manually through the pipe as far down as possible without damaging the wire. Experience with the traversing gear and this particular set up indicates that the measured wall distance is accurate within ± .02 mm. Locating the zero point correctly was the major difficulty when using this procedure.

2.3 Data reduction

The measurements were transferred to punched cards and a computer program (in Fortran IV for the ICL 1901) was used to extract velocities, distances, pressure etc. in the form of tables and plots. The procedure used to obtain the different variables of interest is described in the subsections below.

Density, ρ

Although the flow is practically incompressible the CINA atmosphere was used to obtain the density from the measured pressures, to account for variations in atmospheric pressure and the slightly different pressures at different stations.

Mean velocity from hot wire readings

Figure 5 defines the coordinate system and velocity components. During calibration, constant velocity was established and the centre line velocity determined from Rake B. The hot wire was then traversed to the centre of the pipe in the empty test section and a reading was taken. Each hot wire was calibrated by means of 5 to 24 points covering the test Reynolds number region. A straight line was fitted to each calibration by a least squares method. Higher order fits were also tried but did not improve the accuracy significantly. For small transverse velocities the hot wire was assumed to measure U ($>>$ V, W).

The influence of wall proximity and stem interference is discussed in [7]. As the corrections are not generally applicable, the present data have been left uncorrected.

RMS of the fluctuating velocity

This variable was computed from the corresponding rms voltage by means of the mean velocity calibration curves. In the cases where the transverse mean velocity is negligible when compared to the axial

velocity, this RMS value corresponds to $\sqrt{u'^2}$ where u' is the fluctuating part of the streamwise velocity. In other cases it contains elements of both axial and radial velocity fluctuations and the reading is a measure of intensity only.

Pipe Reynolds number, $Re = \bar{U} D_{pipe}/\nu$

The pipe Reynolds number is computed from the average velocity $\bar{U}$ across the pipe section estimated in the following manner. The measured centre line mean velocity U_e is related to the volume flow velocity $\bar{U}$ by the two equations

$$\frac{\bar{U}}{U_e} = \frac{2n^2}{(n+1)\ (2n+1)} \qquad \text{and} \qquad \frac{n}{2} + \log_{10} n + 0.4 = \log_{10} Re$$

The first expression follows from the assumption of a power law velocity profile in a pipe and the second one is the relation between power law exponent n and Reynolds number validated in [1]. (It is based on Nunner's assumption that $n = 1/\sqrt{f}$ and Prandtl's friction law.)

The average velocity $\bar{U}$ could have been integrated from the measured mean velocity profile, but as [1] showed that the above expressions represent the present flow with reasonable accuracy, and as the pipe Reynolds number accuracy is not very critical, this procedure is considered to suffice for the present purpose.

Friction velocity, $u_\tau = \sqrt{\tau/\rho}$

The friction velocity was computed at the Stations 9 and 12 from the pressure drop between Stations 9 to 11 and Stations 10 to 12, respectively:

$$\tau = \frac{4}{D_{pipe}} \cdot \frac{dp}{dx}$$

The friction velocity $u_\tau = \sqrt{\tau/\rho}$ and the friction Reynolds number is defined: $R_+ = u_\tau D_{pipe}/\nu$.

Nominal velocity profiles

As already mentioned the objective of the present investigation is to determine the local deviations from undisturbed pipe flow due to the presence of a probe in terms of axial mean velocity U and turbulence intensity $\sqrt{\overline{u'^2}}$. It is then essential to be able to describe analytically the "undisturbed" profiles in a way that is consistent with earlier [1] measurements with total pressure rakes and the present with hot wires as described in [7].

Local mean velocity U_N

The main restrictions on the analytic profile equations for $U_N(y)$ is that U_N and dU_N/dy have to be continuous and the overall shape should be consistent with earlier experiments [1] and [7].

During the earlier measurements there were signs that second order effects on the profile could be significant in the pipe flow, as the "constants" in the Law of the Wall indicated a dependence on Reynolds number. A further analysis [7] reveals that the reason may be pressure gradient effects, which in a pipe show up as Reynolds number dependence. Although most of the present measurements are performed at a fixed pipe Reynolds number, the variation in pipe Reynolds number (pressure gradient) may be significant. Besides, comparison with other reference runs at other pipe Reynolds numbers are made easier.

In [1] a power law fit to the data yields exponents in agreement with the Reynolds number trend given by the aforementioned combination of Nunner's and Prandtl's expressions connecting n to f and f to Re respectively. If one assumes that a logarithmic law with a gradient $A(R_+)$ in accordance with Tennekes [8] and a power law of $n(R_+)$ (Nunner-Prandtl) at some point have equal mean velocity gradients dU/dy, then it turns out that this point has a wall distance in the region 14 to 20% of the pipe radius depending on R_+. The condition that the curves join in this point then determines the additive constant $B(R_+)$ in the logarithmic law.

The following equation gives the nominal velocity profile down to $y^+ = 40$:

$$u^+ = A(R_+) \ln y^+ + B(R_+)$$

where $A(R_+) = 3 - 5R_+^{-1/3}$; $B(R_+) = 10.82 - 0.818 \ln R_+$

The wake region is expressed in accordance with Coles' definition, but so that its strength (given by Π) is given as a function of R_+. Using the U_e at Station 12 which is assumed to be unaffected by the presence of the probe, one obtains

$$\frac{U}{u_\tau} = A(R_+)\left[\ln y^+ + 2\Pi(R_+) \sin^2(\pi y/D) + B(R_+)\right]$$

where $\Pi(R_+) = \frac{1}{2}\left[\frac{U_e/u_\tau - B(R_+)}{A(R_+)} - \ln(\frac{R_+}{2})\right]$

If Π is estimated using $n(R_+)$ one obtains a rather significant R_+ variation, as compared to the value of about 0.32 obtained practically independent of Reynolds number by calculating with Coles' values A = 2.439 and B = 5.0. (Changing the value of B to 5.2, as suggested by Brederode and Bradshaw [9], results in a reduction of Π by 0.04.)

Rather few of the present measurements are taken within the viscous sublayer or buffer zone and the main requirement is therefore that the selected expression shall match in u^+ and du^+/dy^+ at $y^+ = 40$. (Deviations from the logarithmic law often are considered to be significant somewhere below $y^+ = 30$ to 50.) A modification of Rannie's [10] expression is chosen:

$$u^+ = C(R_+) \cdot \tanh(y^+/D) \; ; \; C(R_+) = 17.5 - 0.4 \cdot \ln R_+ \; ; \; D = 17$$

(Rannie used C = D = 14.53, matching a logarithmic law with constant A and B at a lower y^+ value.)

The effects of the different choices of assumed velocity profile may be exemplified by Figure 6, showing the situation for Re= 55600. Although the agreement at low y^+ between the $A(R_+)$, $B(R_+)$-line and that obtained by Townsend's [11] equation should be considered a coincidence it illustrates that assuming A and B constant for the present experiment would not be justified.

The velocities computed from the equations involving pressure gradient dependence are considered the nominal mean velocities U_N, and for measurements in the disturbed flow field the measured quantities are divided by the proper local U_N.

3. EXPERIMENTS

3.1 Experiments with empty test section

Before any measurements were made near the cylinders, a series of runs were used to establish a "reference" flow situation over the entire Reynolds number range to be investigated later. Some extra runs of this kind were also made near the end of the tests. The results are summarized in Figure 7. These 14 runs are subject to a more complete discussion in [7], where the profiles are tabulated.

Figure 7 shows that the measured mean velocity profiles in general agree with the assumed one. Least squares curvefits to each profile yield slopes lower than presumed, at about A= 2.2. This is believed to be a result of the uncertain hot wire response in the proximity of the wall.

One of the turbulence profiles measured here has been plotted in Figure 8 for comparison with Laufer's [12] results. The agreement is reasonably good for $y/R > 0.2$; i.e. outside the logarithmic region. Closer to the wall points of Laufer's profile indicate a much higher turbulence intensity than the present. Recent results by Perry and Abell [13] are also shown. They indicate that in a

region $y^+ > 100$, $y/R < 0.1$ the streamwise turbulence intensity is constant. Other profile measurements from the present set up also indicate that the region of deviation from a linear relationship is smaller than the logarithmic region, and for the purposes of the present report it suffices to make a linear curvefit based on points at $0.2 < y/R < 0.95$ and extrapolated across the entire pipe section:

$$\frac{\sqrt{\overline{u'^2}}}{u_\tau} = \chi \cdot (1-y/R) + \omega$$

Least squares fits of the profiles show that both χ and ω have a Reynolds number dependence. For simplicity the values are chosen constant for the measurements near the cylinder ($Re \sim 1.15 \cdot 10^5$)[7].

$$\chi = 1.0$$
$$\omega = 0.65$$

3.2 *Experiments with surface cylinders*

The cylinders were positioned in various locations with the hot wire at fixed streamwise position to give a large number of readings at the stations considered to be of main interest, namely near the leading and trailing edges (See Figure 2). The hot wire was traversed across the entire diameter of the test pipe to obtain information on possible asymmetries arising. For the runs and probe positions considered to be of main interest the traces on the oscilloscope were recorded.

Table gives the overall data of the runs with surface cylinders positioned and the recorded mean velocity and turbulence intensity profiles.

As the information on how the cylinder disturbs the flow is based on hot wire measurements with the assumption that the flow is perpendicular to the hot wire, a few tests were made to ascertain whether or not this was indeed justified. The hot wire was placed in the pipe centreline and rotated till the reading was minimum. A hot wire probe parallel to the flow has a heat loss of about 55%

of that when the wire is perpendicular to the flow [14], which explains the rather high readings obtained. The hot wire was traversed across the pipe section and significant departures from the centreline values would indicate swirl or other inconsistencies in the flow. Three tests were made at the pipe Reynolds number used for most of the measurements, one without a cylinder mounted, one ahead of the cylinder and one in the wake of it. These indicated that one may treat the plane of measurement as a true symmetry plane for the flow.

Most of the experiments concerned the flow around the 19 mm cylinders in fully developed turbulent flow, for which the pipe Reynolds number was held approximately constant with a pipe centreline mean velocity of about 20 m/s. As an aid in estimating the Reynolds number effects a few runs were made at U_e about 10 m/s and a few at much lower velocities with laminar flow. The effect of cylinder diameter was investigated by means of 10 and 5 mm tubes with one measurement in the wake of each.

3.3 Pressure distribution measurements

Although the hot wire measurements established the upstream influence of a surface cylinder and the flow visualization illustrated this effect quite clearly, it was considered desirable also to measure the upstream influence on the static pressure field. Therefore a simple experiment was designed.

A flat plate with a sharp leading edge was mounted in the FFA 0.4 x x 1 metre Building Aerodynamics (BA)-Tunnel. About 1 metre from the leading edge surface cylinders of four different diameters (3, 5, 10 and 19 mm) were mounted along the plate centreline and aligned with the flow. Static pressure taps located in one streamwise and one spanwise row were used and the cylinders were positioned at different locations from run to run, so that the pressure distribution around such an obstacle could be mapped. Most runs were made at a free stream velocity of about 20 m/s, as boundary layer measurements indicated that the flow had a reasonably "turbulent" profile at this velocity with a boundary layer thickness of about 50 mm.

3.4 Flow visualization

As an aid in determining the flow directions both in the centre plane where the magnitude was investigated and elsewhere around the cylinders, it would have been desirable to use for example smoke blown from interior of the surface cylinder in the test pipe. Unfortunately the PVC was non-transparent. Therefore these tests were made in the Low Speed Smoke Tunnel of FFA. In this tunnel the flow is laminar and only very low velocity is available. A magnified plexiglass model of the cylinder was placed on a flat plate. Smoke pictures were taken with the cylinder parallel to the flow and at 30^{o} yaw angle. Of course this can not give any real answer to the question of what the flow pattern is in the fully developed turbulent flow like in the pipe, but one may hope that it at least gives an indication of the magnitude and shape of the flow around a cylinder on a wall.

In order to obtain some information on the surface flow pattern around the cylinder in a turbulent boundary layer additional tests were made in the BA-Tunnel. Cylinders of diameters 10 and 19 mm were positioned 1 metre behind the leading edge of the flat plate as discussed in the previous section. The free stream mean velocity was about 20 m/s, as in the pressure distribution tests. Visualizations were then made by means of oil flow. Even the flow pattern on the cylinder itself was illustrated to some extent by these tests, as shown in the next section.

4. RESULTS

4.1 Mean velocity profiles

Figure 9 shows the measured mean velocity U relative to the nominal mean velocity U_N given by the formulae in Section 3. Contours are given ahead of and behind the cylinder, respectively. Behind the cylinder it can be seen how the velocity gradients rapidly get smaller while it takes more than one cylinder diameter before the wake strength itself decreases significantly.

In Figure 10 an interpretation of all the measured mean velocity profiles has been made, indicating the levels of the ratio U/U_N. It is seen that measured velocities in the centre plane above the cylinder do not show any increase due to blocking until more than one cylinder diameter behind the body. This may be seen as an indication that the flow is primarily forced around the side of the body rather than being displaced vertically. This may be more pronounced when the cylinder is mounted on a flat plate.

The Reynolds number and cylinder diameter effects are illustrated in Figure 11. The profiles for $U_e \sim 10$ and 20 m/s are practically identical, i.e. the Reynolds number effect based on model (cylinder) scale and pipe scale are both too small to be measured. Regarding the diameter effects these are difficult to sort out as the wake behaviour is likely to scale mainly on the cylinder diameter while the profiles were taken for $X_O = 0.45$, i.e. scaled on pipe radius.

4.2 Turbulence intensity profiles

Figures 12 to 14 show the turbulence intensities from the profiles. They are given as RMS/u_τ to indicate the effects of the vertical velocities in certain regions ahead of and behind the cylinder. Here u_τ is the undisturbed friction velocity far from the surface cylinder. As could be expected the turbulence intensity has a large value where the mean velocity gradients are large. Behind the cylinder the fluctuations are seen to be progressively stronger downstream in the wake, but as shown in Figure 13 the measured intensity is significantly larger than in the "nominal" case within one half cylinder diameter from it. An indication of a Reynolds number effect on the turbulence level all through the cross section is indicated in Figure 14, but the disturbance of the cylinder appears to be Reynolds number independent. As in the case of the mean velocities, it is again difficult to draw conclusions on any diameter influence.

4.3 Oscilloscope traces

In the Figures 15, 16 and 17 a selection of relevant oscilloscope traces of the signal are given. Figure 15 shows records from ahead of the cylinder and Figure 16 presents data from two stations behind the cylinder. It is seen that the centreline signal is unaffected by the surface cylinder presence, while the magnitude of the variations agree approximately with that expected near the cylinder. There does not seem to be any definite low frequency periodicity in the fluctuations. Figure 17 gives the signals from a station ahead of the cylinder at the two different Reynolds numbers, corresponding to U_e= 10 or 20 m/s. The scales on the pictures are Volts/unit which corresponds to a velocity fluctuation of about 3.3 ms^{-1}/unit. It appears that at the lower Reynolds number the highest frequency oscillations are much weaker and show up just as a ripple on the low frequency signal.

4.4 Pressure distribution

The Figures 18 and 19 show the most important results from the pressure distribution experiments. Figure 18 gives an overall map of the pressure disturbance caused by the presence of the cylinder. It is evident that the largest pressure deviations are concentrated to a rather small region along the centreline just ahead of the cylinder. The disturbance is rather weak on the sides, which is important in positioning Preston tubes relative to static holes. It should be observed that even the 19 mm tube, which here occupied a region much larger than the logarithmic region, showed results in accordance with those of the smaller cylinders. Figure 19 shows experimental results along the centreline compared with a simple calculation. The simple inviscid calculation has been performed by treating the cylinders as a three-dimensional source located at x= 0, y= D/2. The wall presence is accounted for by an image source at x= 0, y= -D/2. The source strength is determined by forcing the wake of the upper source to go through y= D far downstream when a

uniform free stream is imposed. Figure 19 shows the results of this simple exercise and one may conclude that outside the region of about one diameter from the cylinder the local pressure is well represented by simple considerations like the one above.

4.5 *Flow visualization*

In Figure 20, oil flows on the flat plate are shown for the 19 mm cylinder. The rapid divergence of surface streamlines ahead of the cylinder can be seen, as well as the separation line about one diameter ahead of the leading edge. The strongly perturbed region is seen to extend about one cylinder diameter to both sides of the obstacle. A rather large separated area can be seen just behind the cylinder trailing edge. This flow pattern with one or more horseshoe vortices is nothing unexpected; the different shapes occurring have been discussed earlier, for example in [15]. The main difference is that most investigations concern cylinders with the axis normal to the wall, rectangular blocks etc.; whereas the present configuration has concave corners near the wall. The two vortices in the corners formed by the cylinder and wall appear to feed material into the separation bubble from behind. The wake development in the near body and the far body regions can also be seen in the figure. The effect of cylinder size is demonstrated in Figure 21, where the smallest cylinder extends to about 10% of the local boundary layer thickness. There appears to be a small effect of cylinder diameter in the front region. The wakes of the different cylinders are somewhat different (Figure 22). The 5 and 10 mm tubes have no distinct separation bubble at the rear, unlike the 19 mm tube, but apart from this the relative wake size and the general flow development appears to be similar. Figure 23 shows the flow pattern on the cylinder itself. At the front it appears in the first picture a small separated region extending only some tenth of a cylinder diameter downstream. The other picture demonstrates another interesting feature; the two vortices formed under the cylinder at the front. They seem to start on the cylinder wall and from the earlier figures it appears furthermore that their traces on the surface extend outwards until they are entrained in the horseshoe vortex.

Figure 23 also has a side view of the 19 mm cylinder. In the corner between the wall and the cylinder there is a distinct region where the horseshoe vortex is located.

Some stereo photographs have been taken of the oil flows on the 19 mm cylinder in the turbulent boundary layer (Figure 24, top) and of smoke visualizations in potential flow near a large plexiglass cylinder (Figure 24, bottom). It should be noted that stereo lenses are needed to see the photographs in three dimensions. In the smoke photographs streamlines can be seen to enter the mouth of the cylinder, whereupon they suddenly turn outward again.

4.6 Pressure drop

This part treats the drag of the surface cylinder in pipe flow. From the experiments performed earlier [1], data are available on the loss of static pressure due to the presence of the cylinder. The data were obtained as indicated in Figure 25 in the form of a displacement of the pipe static pressure line. This displacement is assumed to consist of

- Form drag on the cylinder itself (Profile and skin friction).
- Change in skin friction drag on the pipe walls.

In obtaining the measurements needed for the computations two of the inclined manometers were used for different parts of the pipe, so that static pressure ahead and aft of the Preston tube were taken from different manometers. To correct for this one of the pressure was recorded on both manometers and the values deduced were compared. One of the two sets of measurements was then shifted by this amount to align the "undisturbed" pressures. The remaining shift then represents the pressure drop due to cylinder presence dp_{pr}; note that in [1] the uncorrected values were printed. This correction procedure is of course questionable and is subject to scatter and bias. In order to eliminate or reduce the systematic errors a series of runs with empty test section was used.

Figure 26 shows the ratio of pressure drop to dynamic pressure dp_{pr}/q plotted versus Reynolds number for different dylinder diameters. In the figure no correction has been made for systematic error, and a line has been drawn corresponding to $dp_{pr} = 3\ N/m^2$ to indicate that data of lower magnitude are questionable. (In those cases the corrections to individual measurements are comparable with the measurement itself.)

This also means that only data from [1] on the three cylinders used here, of diameters 5, 10 and 19 mm, give results of acceptable accuracy. It is natural to try and express the drag of the surface cylinder in wall variables, although the 19 mm body extends far outside the wall region. Expressing the drag coefficient as $C_D^+ = dp_{pr}/\frac{\rho}{2} u_\tau^2$ the results for the different diameters are shown in Figure 27.

In the normal context of $C_D = D/\frac{1}{2} \rho U_e^2$ with U_e being the centreline mean velocity, this becomes:

$$\frac{C_D}{C_f} = \frac{C_D^+}{2} \left(\frac{D}{D_{pipe}}\right)^2$$

From the figure it appears that the cylinders extending outside the logarithmic region have a comparably larger drag than the smaller cylinders.

At the beginning of this section (4.6) the measured pressure drop was assumed to consist of drag on the cylinder itself and influence on the pipe walls by blockage etc. To obtain an order of magnitude estimate for the blockage effects, one may assume an equivalent body equal to the cylinder cross section area and affecting a length three times the cylinder length. It turns out that the resulting increase in skin friction is practically negligible.

5. CONCLUSIONS

The objective of the present study is to investigate the flow conditions near Preston tubes. For practical reasons this has been accomplished with surface cylinders of a larger scale relative to the boundary layer thickness, but the tests should nevertheless give a correct answer to various questions of interest.

- The Preston tube gives rise to a flow pattern much the same as that of other obstacles attached to a surface and immersed in a boundary layer [15], i.e. a horseshoe vortex is formed which embraces the obstacle's front and sides and trails off into the wake.

- The velocity measurements indicate that a secondary vortex is present in the frontal area more than one diameter upstream. In contrast to the main vortex this secondary vortex lifts up from the surface, and is not seen in the oil flows.

- A separated area extends about one diameter upstream and to the sides of the tube.

- The disturbance in static pressure extends more than seven diameters upstream, and is equivalent to the disturbance due to a source in the centre of the front plane and its image in the wall. With uniform flow the required source strength is such that the limiting surface corresponds to the tube cross section far downstream.

- The drag due to the cylinder corresponds to less than 5 % of the Preston tube dynamic pressure for cylinders located within the logarithmic region, and considerable larger for larger cylinders.

- From the present experiments it appears that it is preferable to locate the corresponding static pressure tap to one side of the Preston tube even in zero or very small pressure gradients. Two or three diameters transverse distance is sufficient to make the pressure disturbance negligible.

- In the literature the maximum permissible Preston tube diameter is often argued to be the logarithmic region thickness. From the present experiments this appears to be a reasonable but rough estimate, and it should be born in mind that the flow is distorted far outside the logarithmic region even for tubes of permissible size. The effects on the Preston tube measurements will nevertheless be small in most cases.

6. REFERENCES

[1] Bertelrud, A. Pipe flow calibration of Preston tubes of different diameters and relative lengths including recommendations on data presentation for best accuracy. Aero. Res. Inst. Sweden (FFA) Report 125 (1974).

[2] MacMillan, F.A. Experiments on pitot-tubes in shear flow. ARC R & M 3028 (1956).

[3] Dhawan, S. Vasudeva, B.R. The pitot tube displacement effect in boundary layer flows. J of The Aeronautical Society of India, Vol. 11, No 1 (Feb. 1959), pp 1-18.

[4] Allen, J.M. Pitot-probe displacement in a supersonic turbulent boundary layer. NASA TN D-6759 (1972).

[5] Dudziniski, T.J. Krause, L.N. Effect of inlet geometry on flow-angle characteristics of miniature total-pressure tubes. NASA TN D-6406 (1971).

[6] Fargie, D. Martin, B.W. Developing laminar flow in a pipe of circular cross-section. Proc. Roy. Soc. (London) A. 321 (1971), pp 461-476.

[7] Bertelrud, A. Undersökning av strömningen i ett 10.5 cm kalibreringsrör. (In Swedish). (To be published).

[8] Tennekes, H. Outline of a second-order theory of turbulent pipe flow. AIAA Journal, Vol. 6, No 9 (Sep. 1968), pp 1765-1770.

[9] Brederode, V.de Bradshaw, P. A note on the empirical constants appearing in the logarithmic law for turbulent wall flows. Imperial College Aero. Report 74-03 (Feb. 1974).

[10] Rannie, W.D. Heat transfer in turbulent shear flow. J. Aero. Sci., Vol 23, No 5 (May 1956), pp 485-489.

[11] Townsend, A.A. Equilibrium layers and wall turbulence. J. Fluid Mech., Part 1 (Aug. 1961), pp 97-120.

[12] Laufer, J. The structure of turbulence in fully developed pipe flow. NACA Report 1174 (1954).

[13] Perry, A.E. Abell, C.J. Scaling laws for pipe-flow turbulence. J. Fluid Mech., Vol 67, Part 2 (1975), pp 257-271.

[14] Doebelin, E.O. Measurement systems: Application and design. McGraw-Hill Kogakusha, Ltd, Tokyo, (International Student Edition) (1966), p 460.

[15] Sedney, R. Kitchens, C.W., Jr. The structure of three-dimensional separated flows in obstacle, boundary layer interactions. AGARD CPP-168 (May 1975).

ACKNOWLEDGEMENTS

Thanks are due to Professor T.K. Fannelöp, Norges Tekniske Högskole Trondheim, and Mr. D.A. Humphreys for the many suggestions during the work. Thanks are also due to Mr. R. Larsson for work with the experiments and Miss I. Engström for the typing and drawing of figures.

SYMBOLS

A, $A(R_+)$	Law-of-the-wall parameter
B, $B(R_+)$	Law-of-the-wall parameter
$C_D = \frac{dp_{pr}}{\frac{\rho}{2} U_e^2}$	drag coefficient in outer scales
$C_{D_+} = \frac{dp_{pr}}{\frac{\rho}{2} u_\tau^2}$	drag coefficient in wall scales
$C_f = \frac{\tau}{\frac{\rho}{2} U_e^2}$	local skin friction coefficient
$C_p = \frac{p}{\frac{\rho}{2} U_e^2}$	pressure coefficient, outer scales
$C_{p_*} = \frac{p_*}{\frac{\rho}{2} u_\tau^2}$	pressure coefficient, wall scales
D	cylinder diameter, constant in Rannie's Law of the wall
D_{pipe}	pipe diameter
dp_{pr}	pressure drop due to Preston tube (see Figure 25)
$f = \frac{\tau}{\frac{\rho}{2} \overline{U}^2}$	friction factor
L	cylinder length
n	power law exponent
p	static pressure
p_*	$p_{disturbed} - p_{undisturbed}$
q	dynamic head
R	pipe radius
$Re = \frac{\overline{U} D_{pipe}}{\nu}$	Reynolds number (in pipe)
RMS, rms	root-mean-square of the fluctuating velocity (hot wire)
$R_+ = \frac{u_\tau D_{pipe}}{\nu}$	friction Reynolds number of the pipe

U, u'	local mean and fluctuating velocity along pipe axis
U_e	free stream mean velocity, in pipe centreline velocity
$\overline{U}$	average velocity across pipe cross section
U_N	nominal (undisturbed) local mean velocity
$u_\tau = \sqrt{\frac{\tau}{\rho}}$	friction velocity
$u^+ = \frac{u}{u_\tau}$	non-dimensional velocity
V, v'	local mean and fluctuating radial velocity
W, w'	local mean and fluctuating transverse velocity
x	streamwise distance
$X = x/R$	non-dimensional streamwise distance, zero at leading edge
$X_o = x/R$	non-dimensional streamwise distance, zero at trailing edge
y	wall distance
$y^+ = \frac{u_\tau y}{\upsilon}$	non-dimensional wall distance
z	transverse distance
υ	kinematic viscosity
Π	parameter in Coles' wake law
ρ	density
τ	surface shear stress
χ	constant
ω	constant

Coordinate system and velocity components are defined in Figure 5.

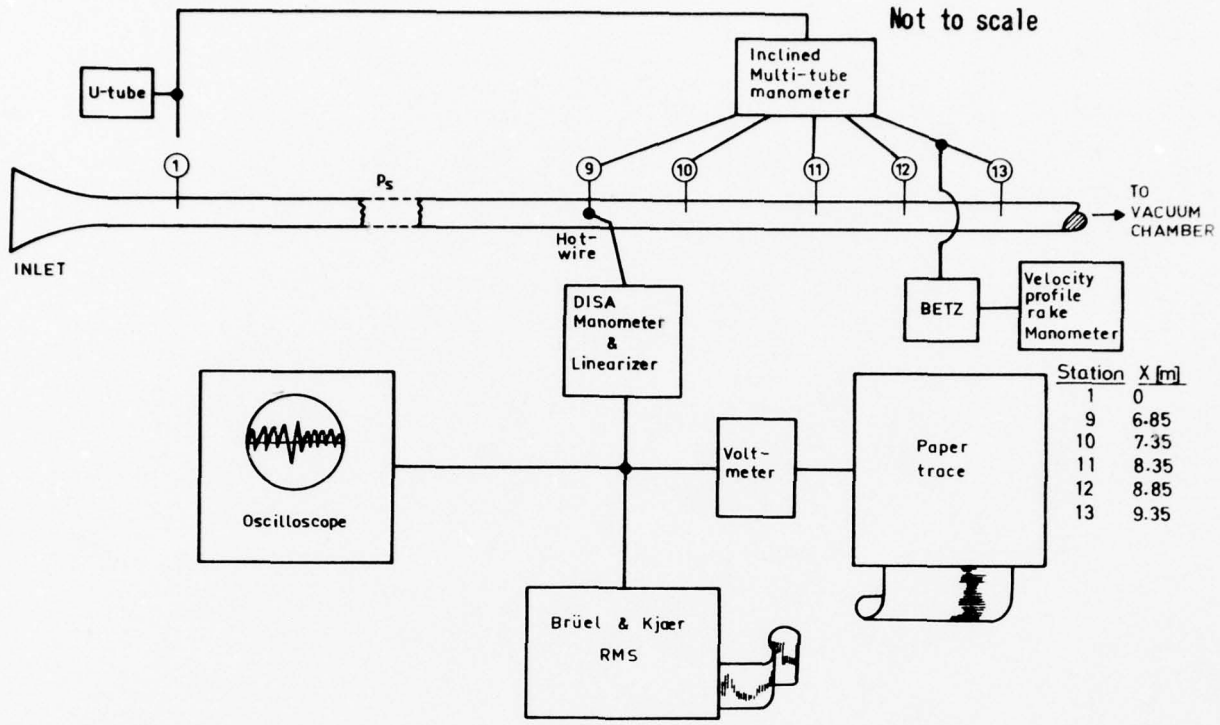

Figure 1. Experimental rig with instrumentation. Pipe diameter 10.5 cm. Details are given in [1].

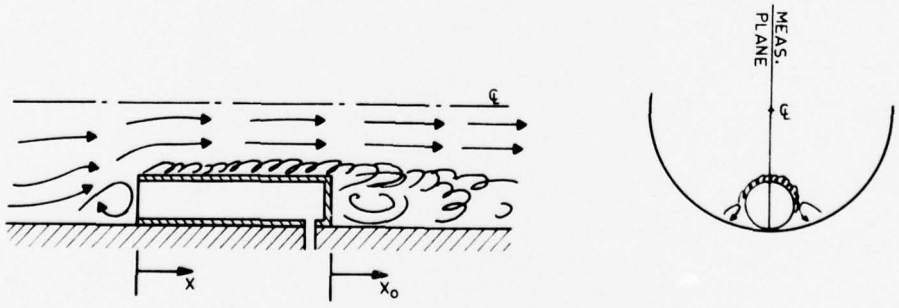

Figure 2. Measurement configuration and definition of streamwise coordinates X and X_o both made non-dimensional by scaling by the pipe radius R.

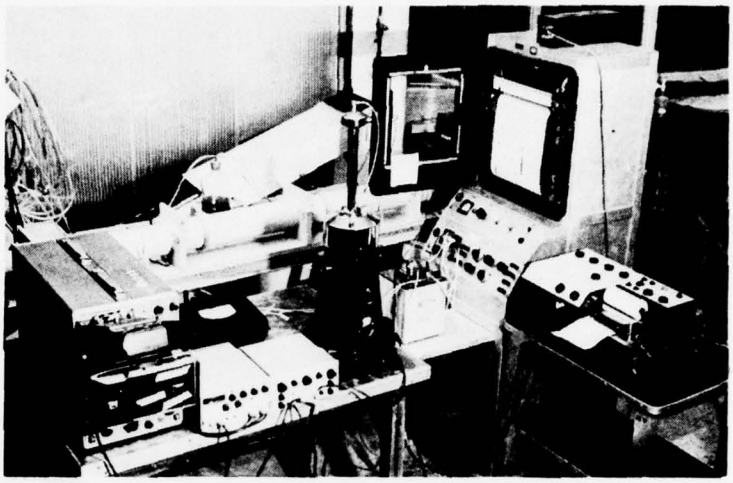

Figure 3. Instrumentation. Oscilloscope with camera, DISA anemometer and linearizer, Betz manometer, paper trace and Brüel & Kjær Level recorder.

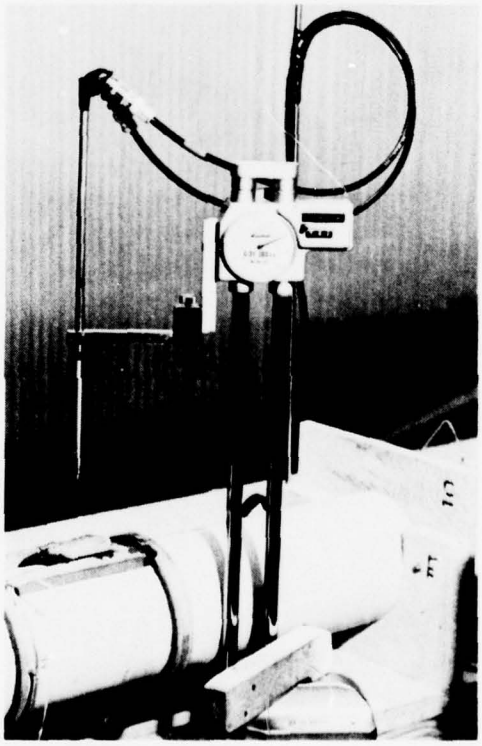

Figure 4. Traversing gear and hot wire with shield removed.

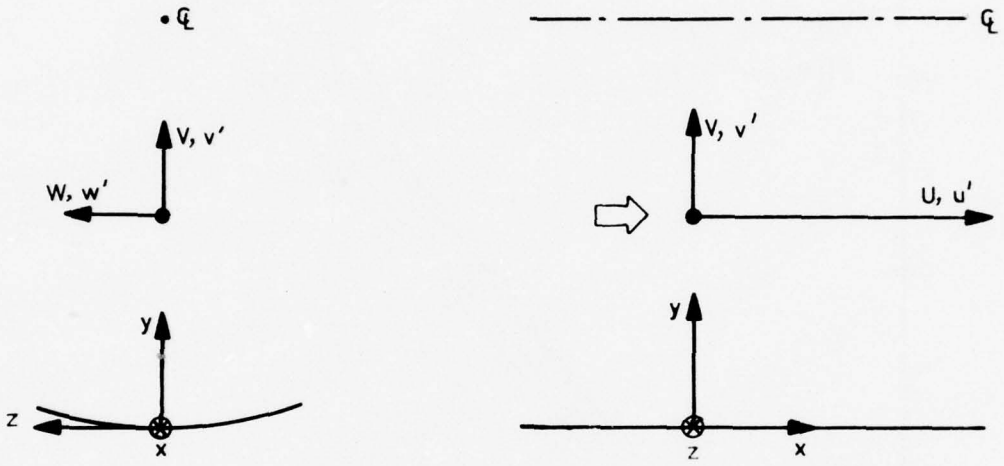

Figure 5. Definition of coordinate systems x, y, z, mean velocity components U, V, W and fluctuating velocity components u', v', w'.

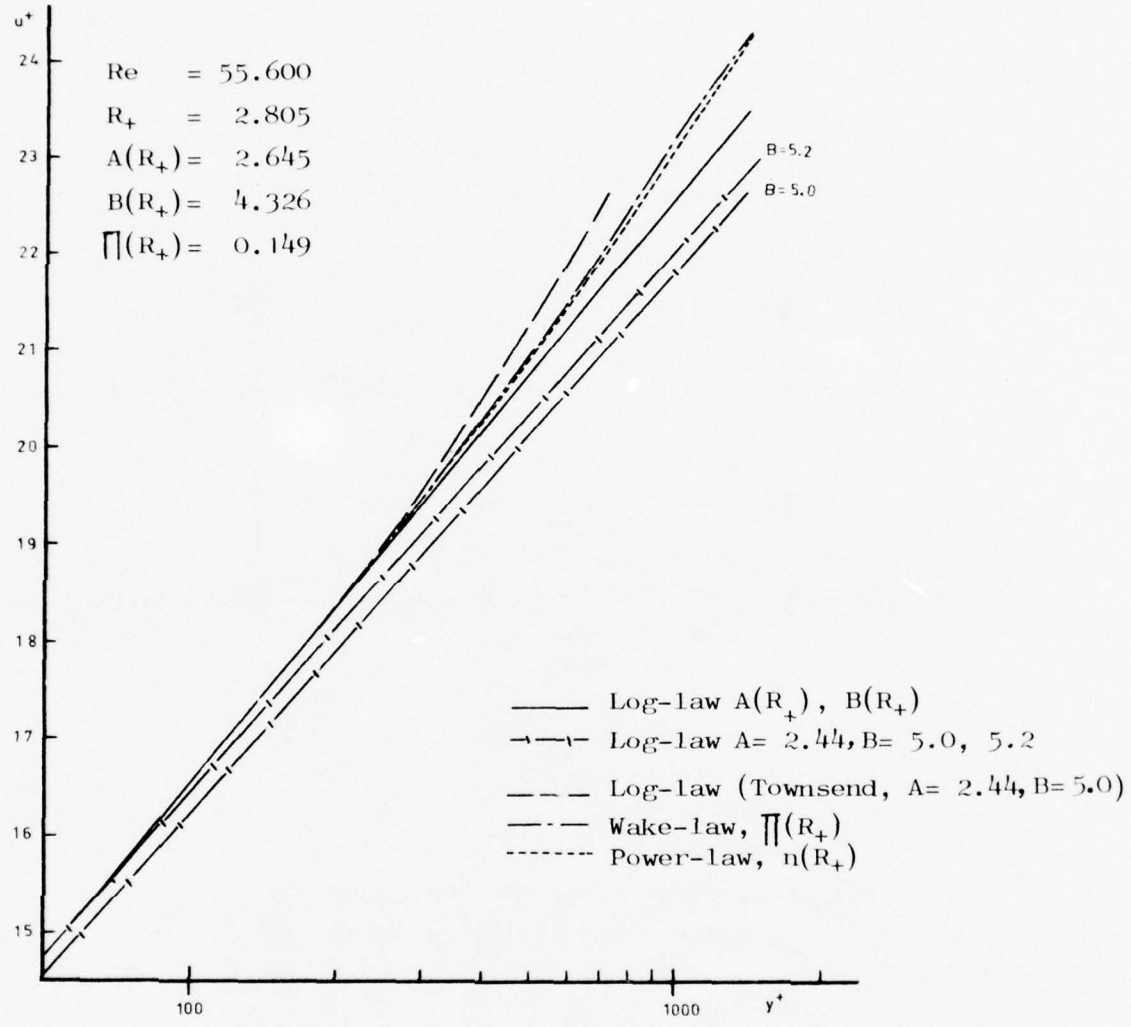

Figure 6. Velocity profiles in pipe flow at $R_+ \approx 2.805$.

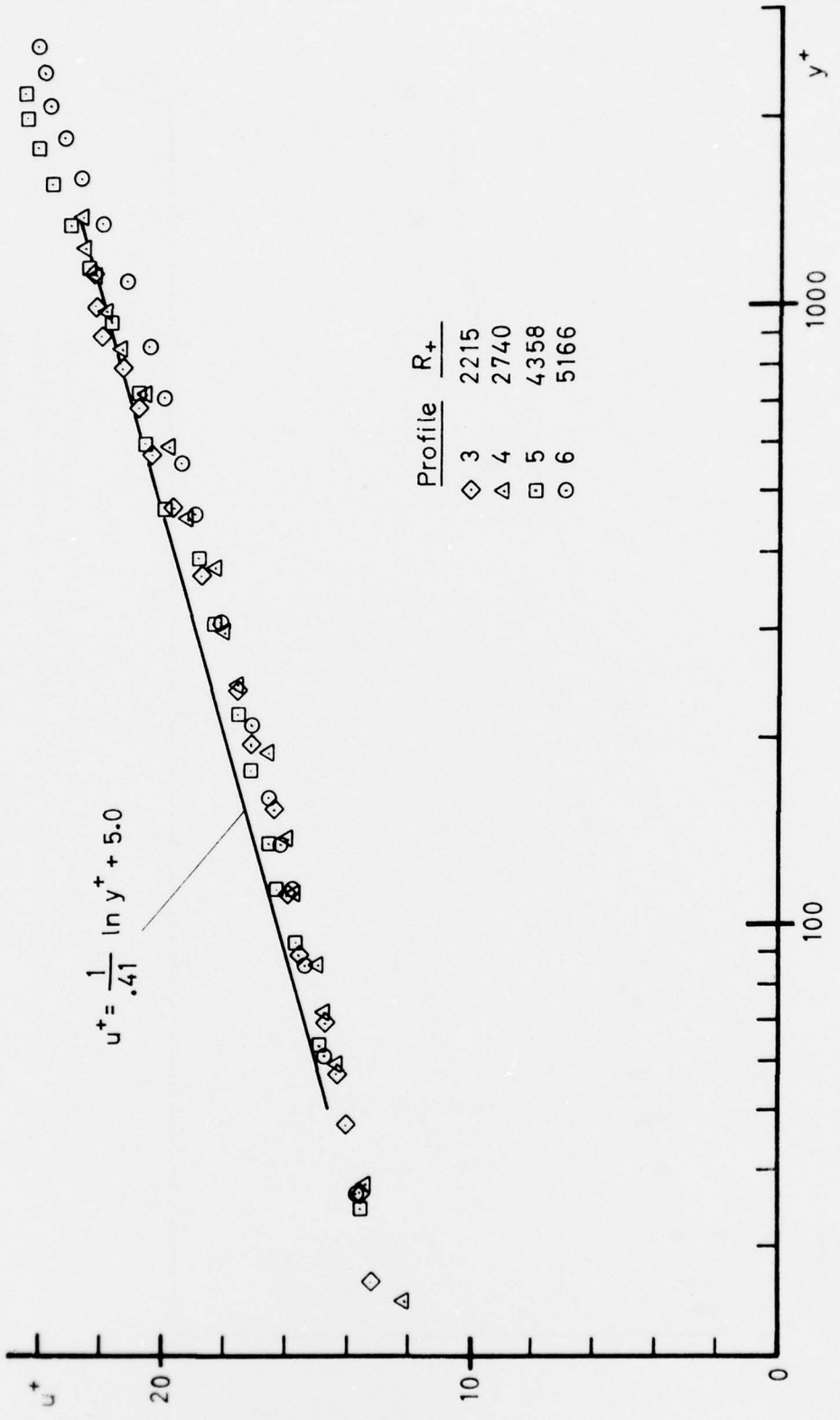

Figure 7. Four velocity profiles measured by hot wire, empty test section. No correction for wall proximity applied.

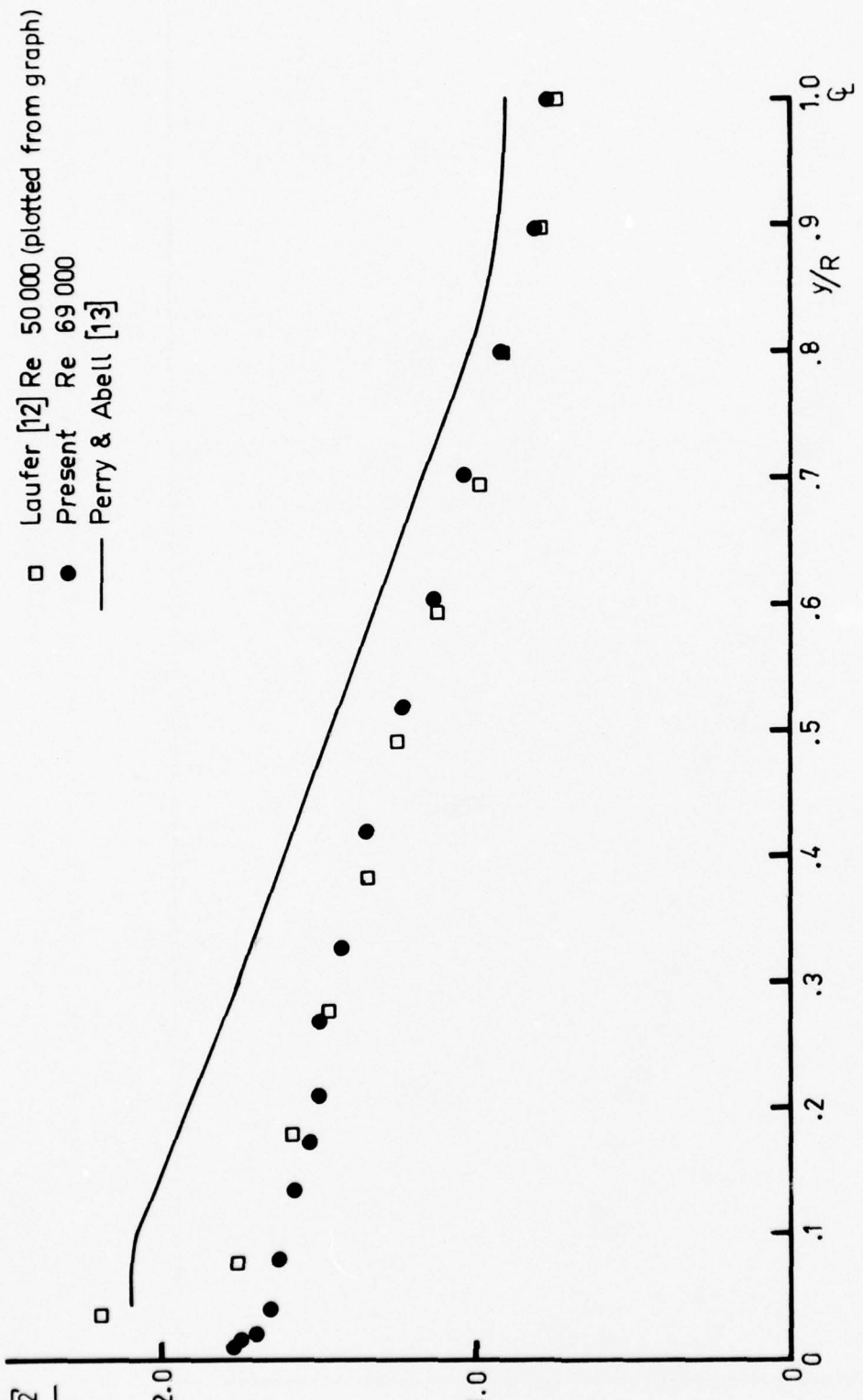

Figure 8. Example of turbulence intensity distribution across the pipe. Note that present calibration is static, while that in [13] is dynamic.

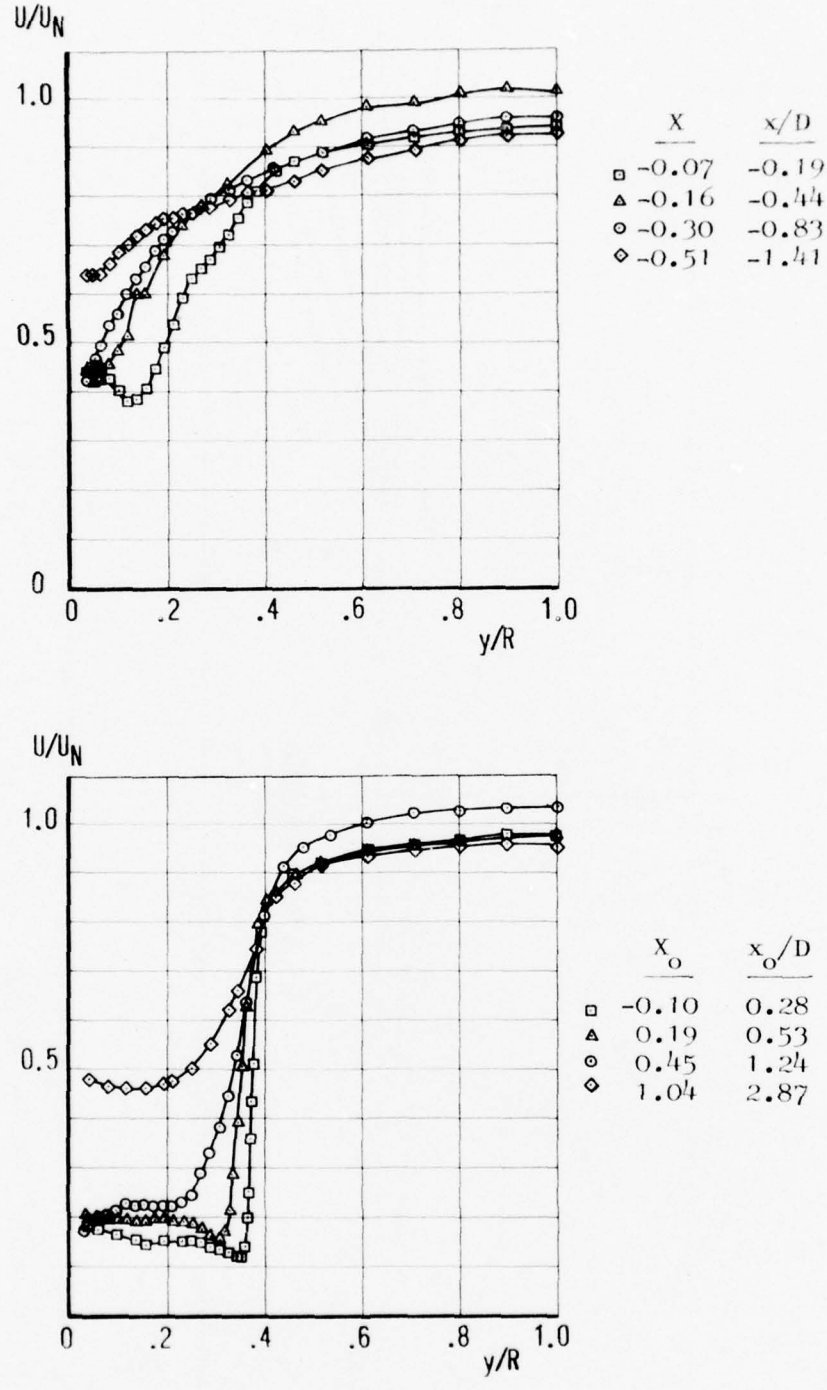

Figure 9. Mean velocity deviations at stations ahead of and behind the surface cylinder.

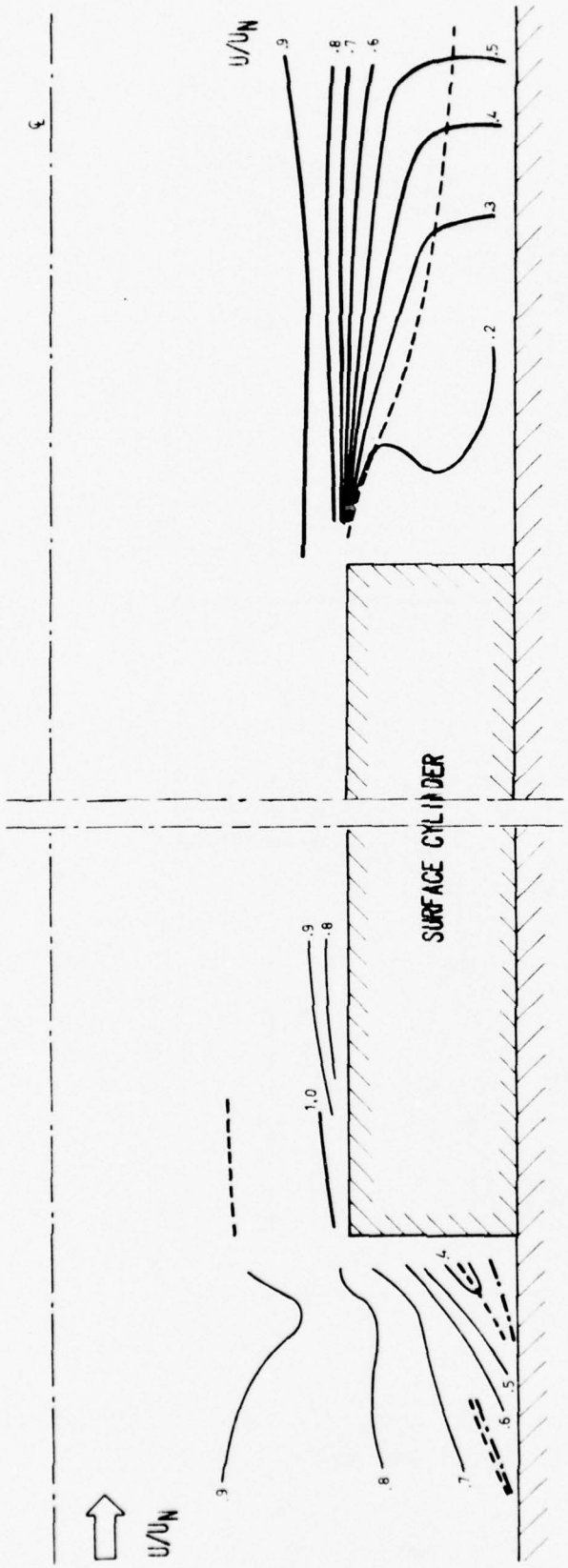

Figure 10. Mean velocity levels. An interpretation of the measured profiles.

	D	$U_e \sim$	x_o/D
-------	5 mm	20 m/s	4.72
— — —	10 "	20 "	2.36
— · —	19 "	10 "	1.24
———	19 "	20 "	1.24

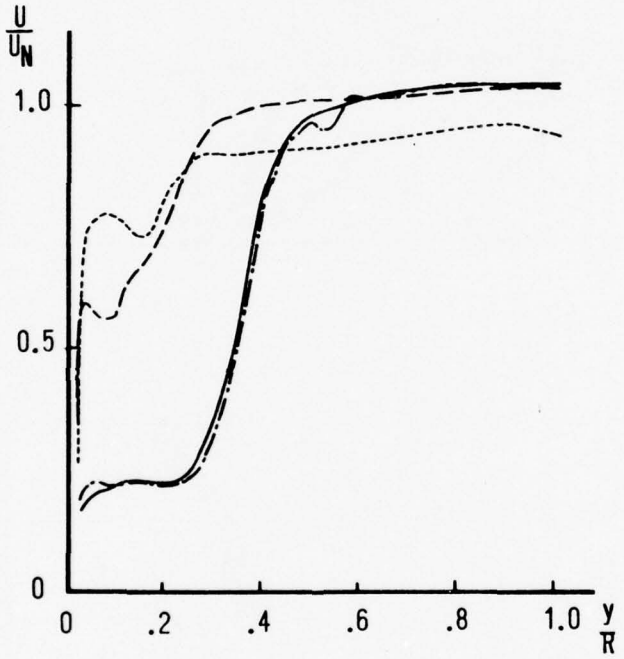

Figure 11. Effect of cylinder diameter and Reynolds number on mean velocity deviations at a distance 45% of R downstream of the cylinder.

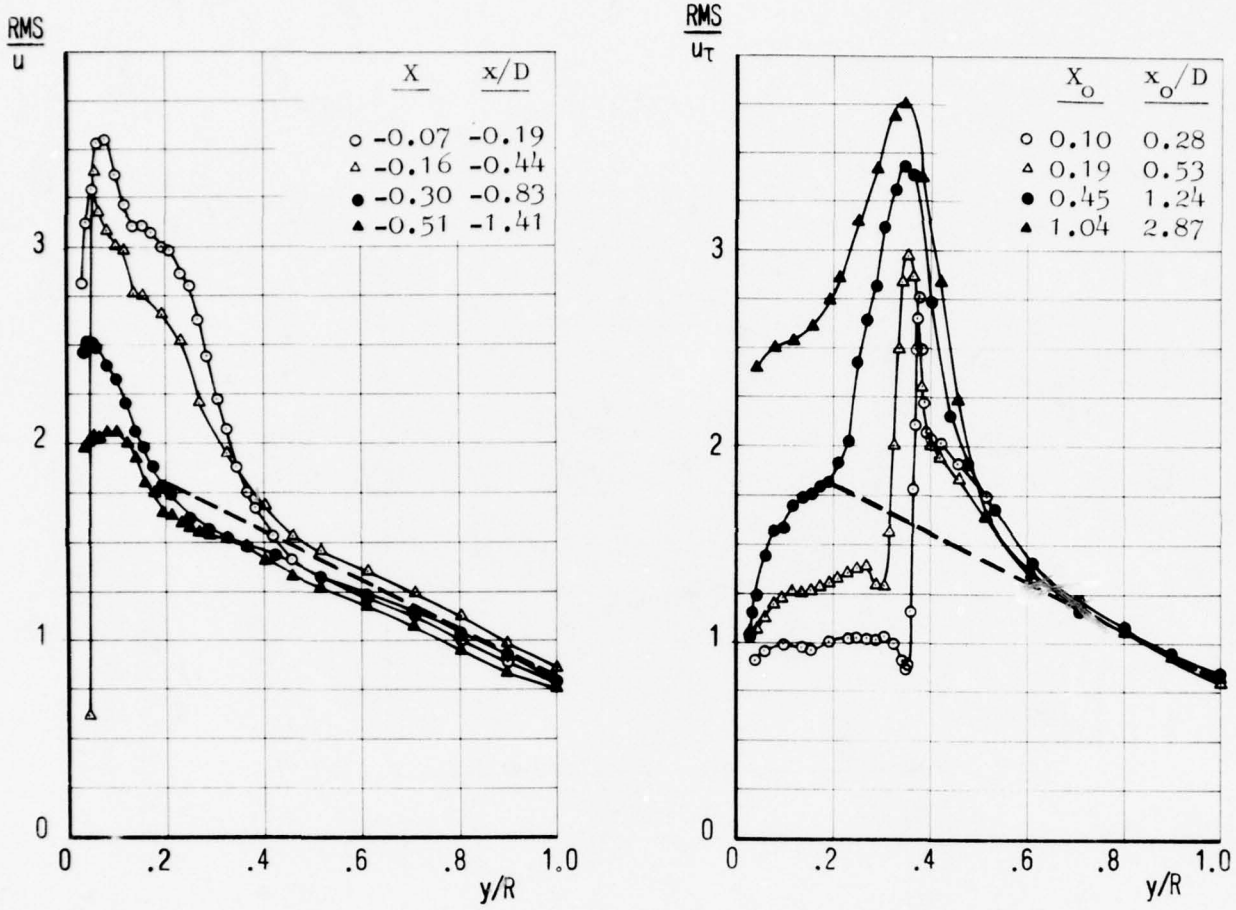

Figure 12. Measured turbulence intensities at stations ahead of and behind the surface cylinder. — — — nominal (undisturbed) distribution outside logarithmic region.

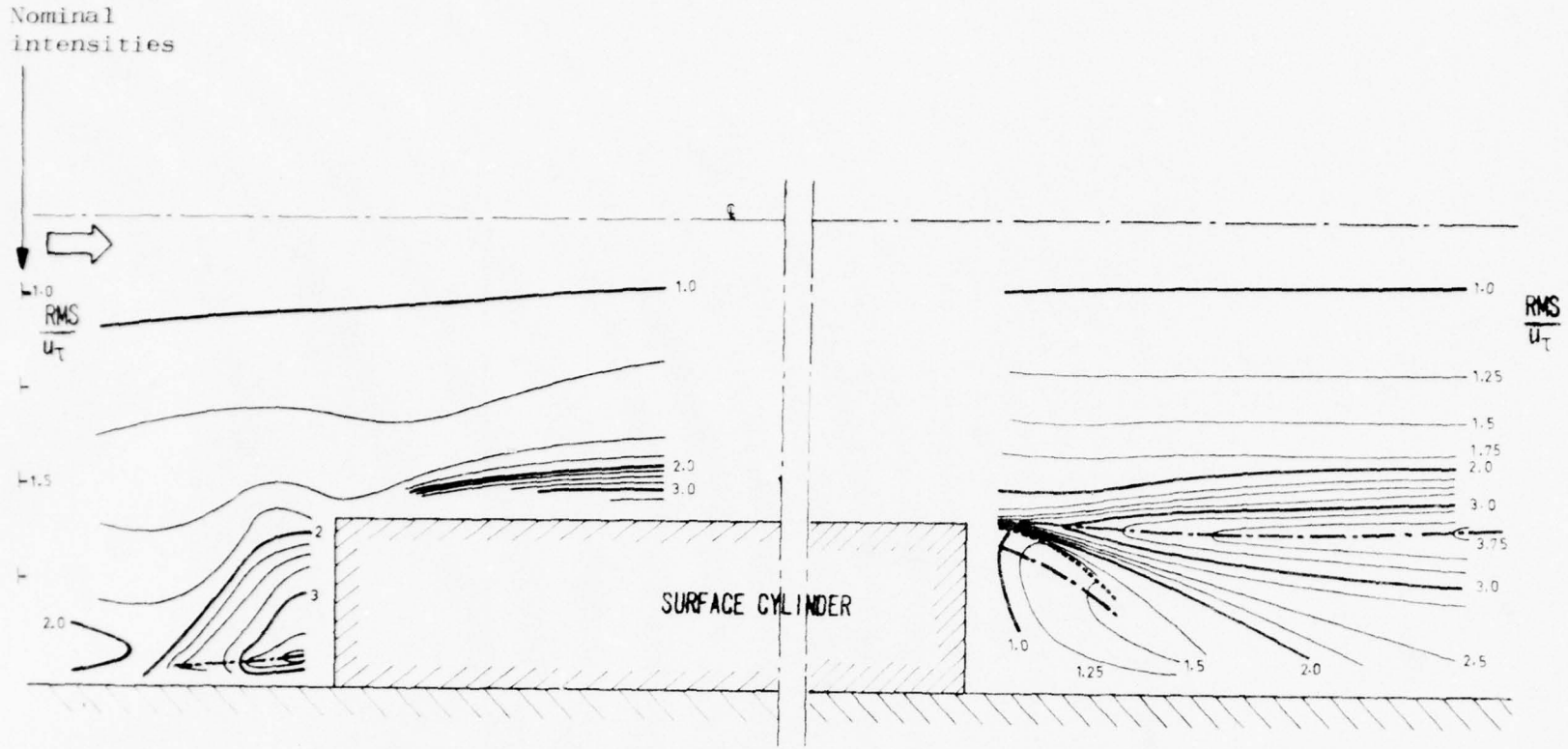

Figure 13. Measured turbulence intensities around the cylinder. An interpretation of the measured profiles. Values to the left are nominal (No cylinder).

——·—— Maximum ------- Minimum

	D	$U_e \sim$	x_o/D
-------	5 mm	20 m/s	4.72
— — —	10 "	20 "	3.36
— · —	19 "	10 "	1.24
———	19 "	20 "	1.24

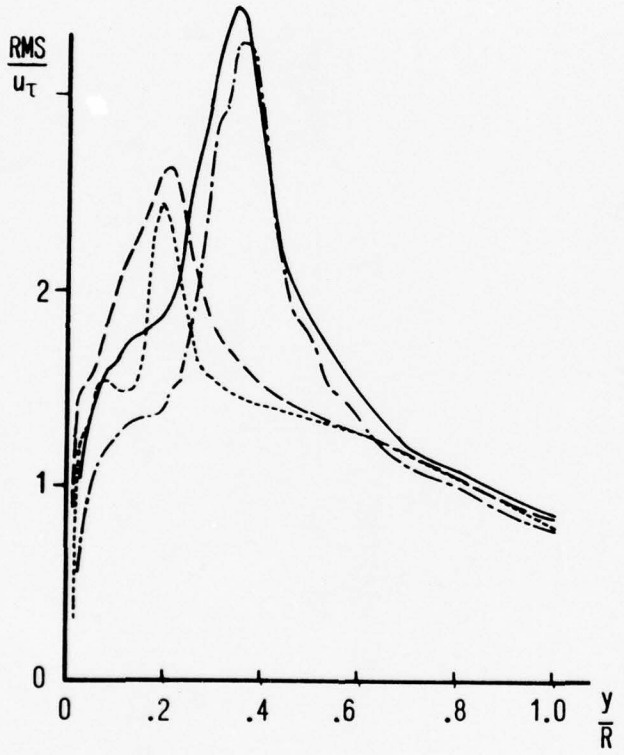

Figure 14. Cylinder diameter and Reynolds number effect on turbulence intensities at a distance 45 % of R downstream of the cylinder.

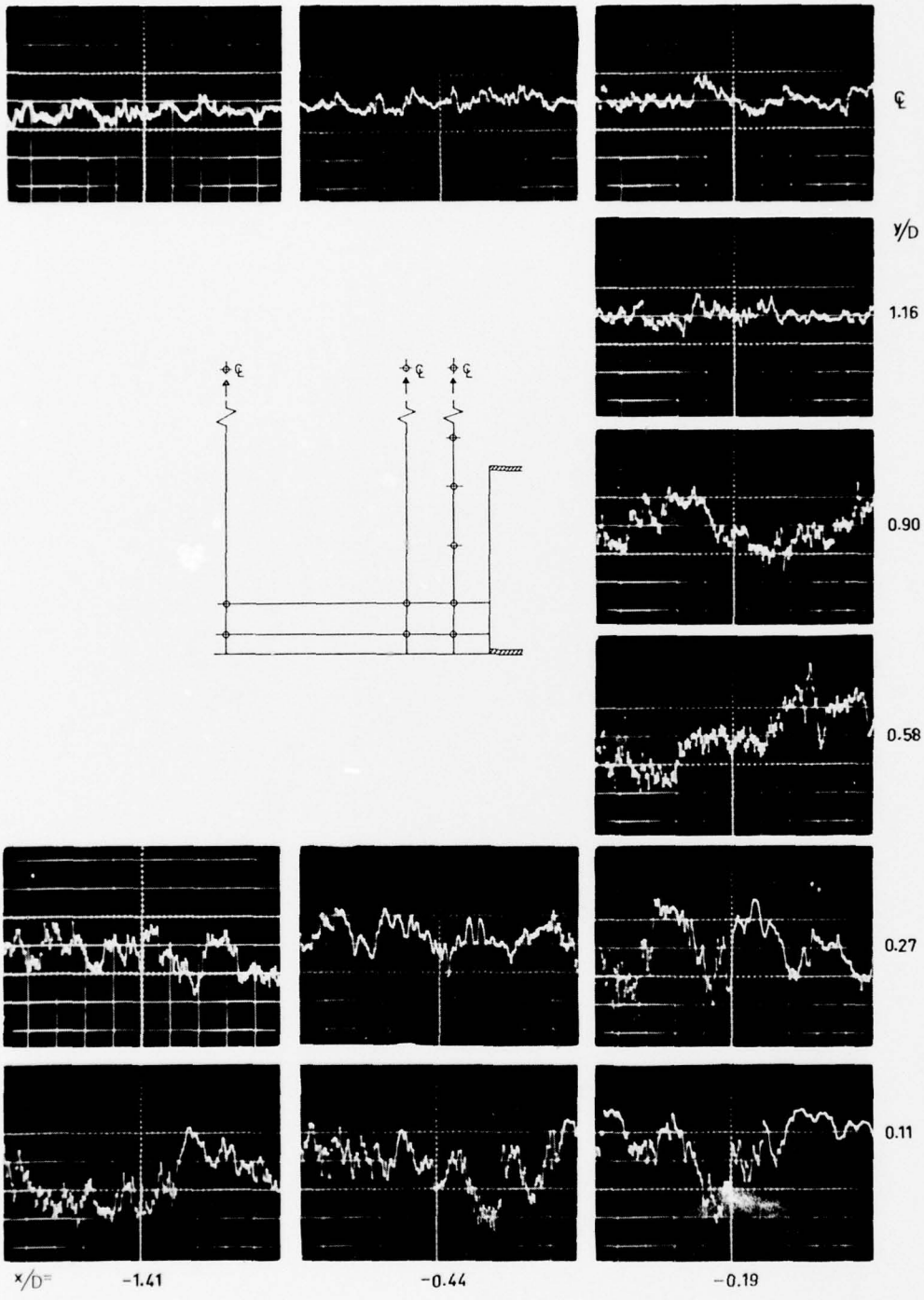

Figure 15. Oscilloscope pictures ahead of cylinder.

Scales: Vertical axis 1 Volt/unit
Horizontal axis 2 msec/unit

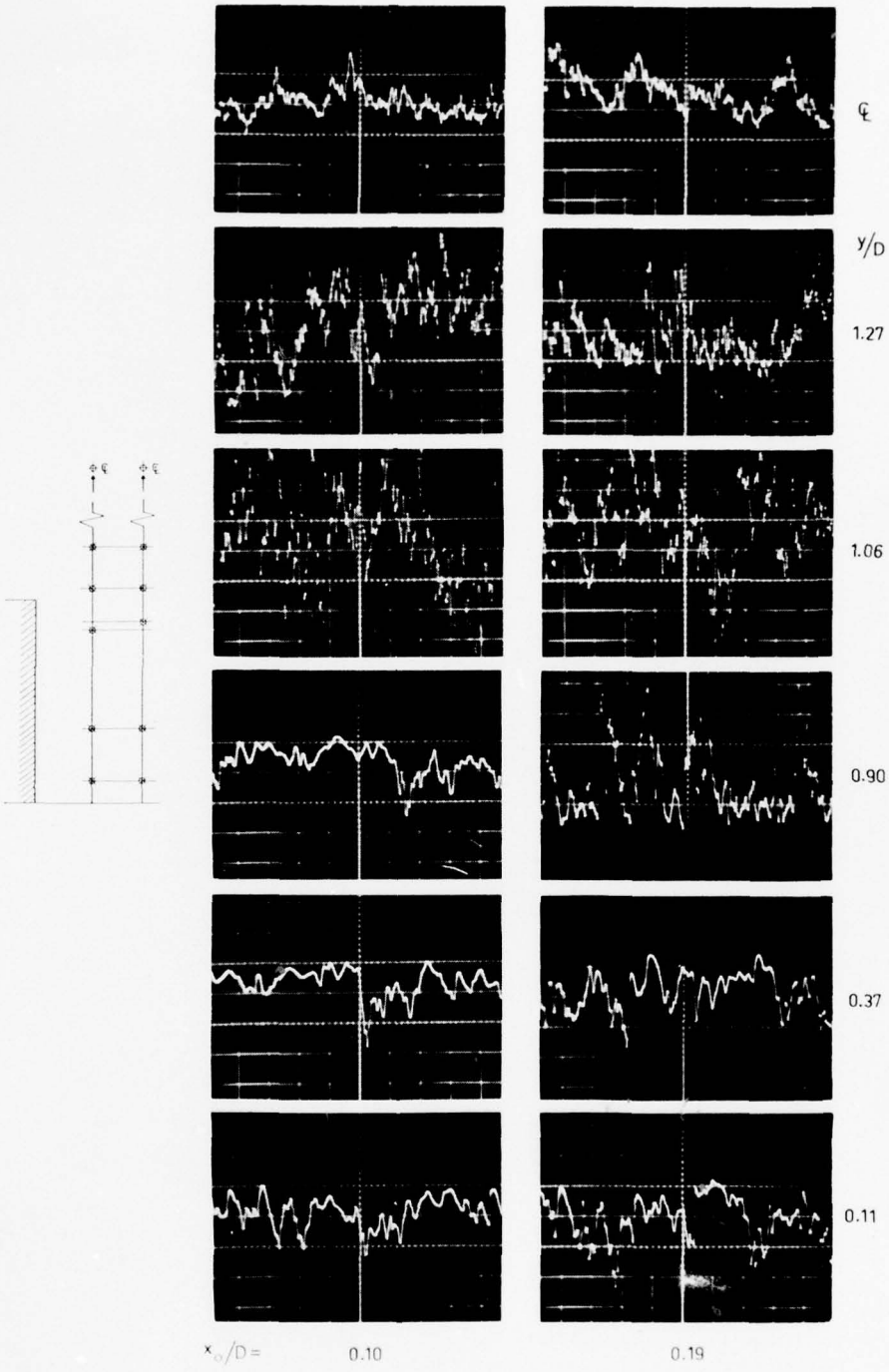

Figure 16. Oscilloscope pictures behind the cylinder.
$U_e \sim 20$ m/s.
Scales: Vertical axis 0.5 Volt/unit
Horizontal axis 2 msec/unit

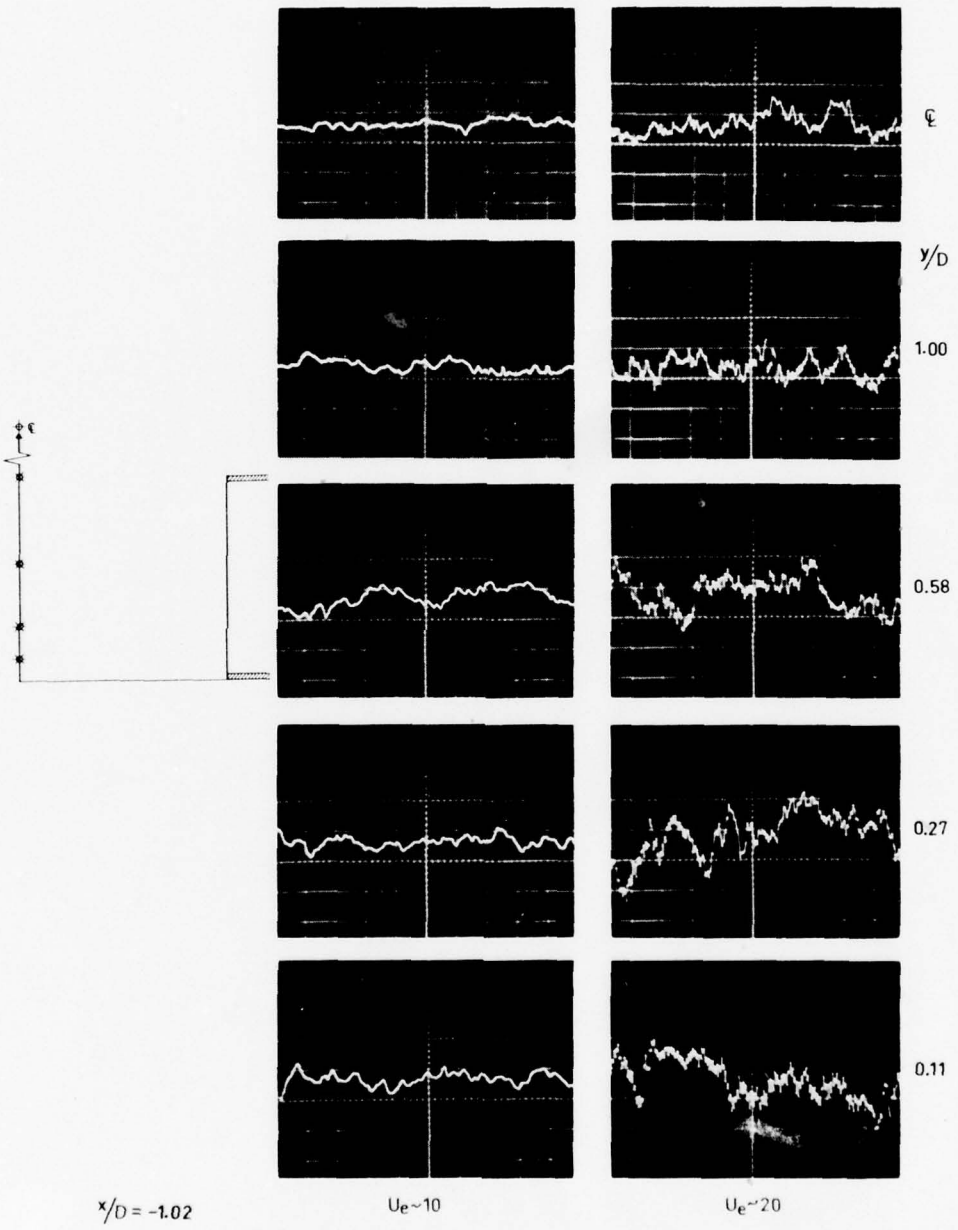

Figure 17. Reynolds number effect.

Scales: Vertical axis 1 Volt /unit
Horizontal axis 2 msec/unit

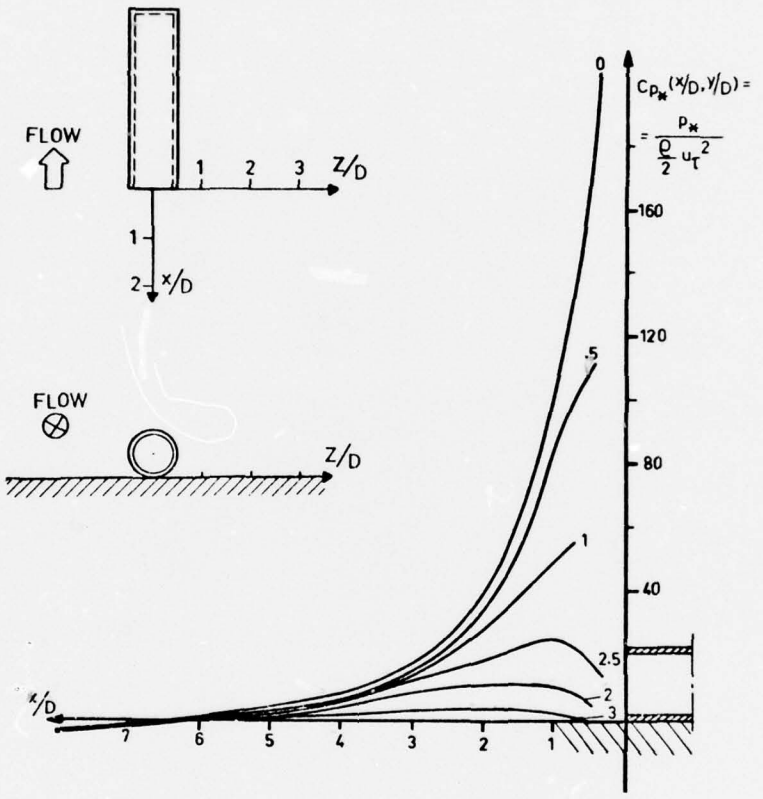

Figure 18. Pressure distribution ahead of a surface cylinder at different transverse position.

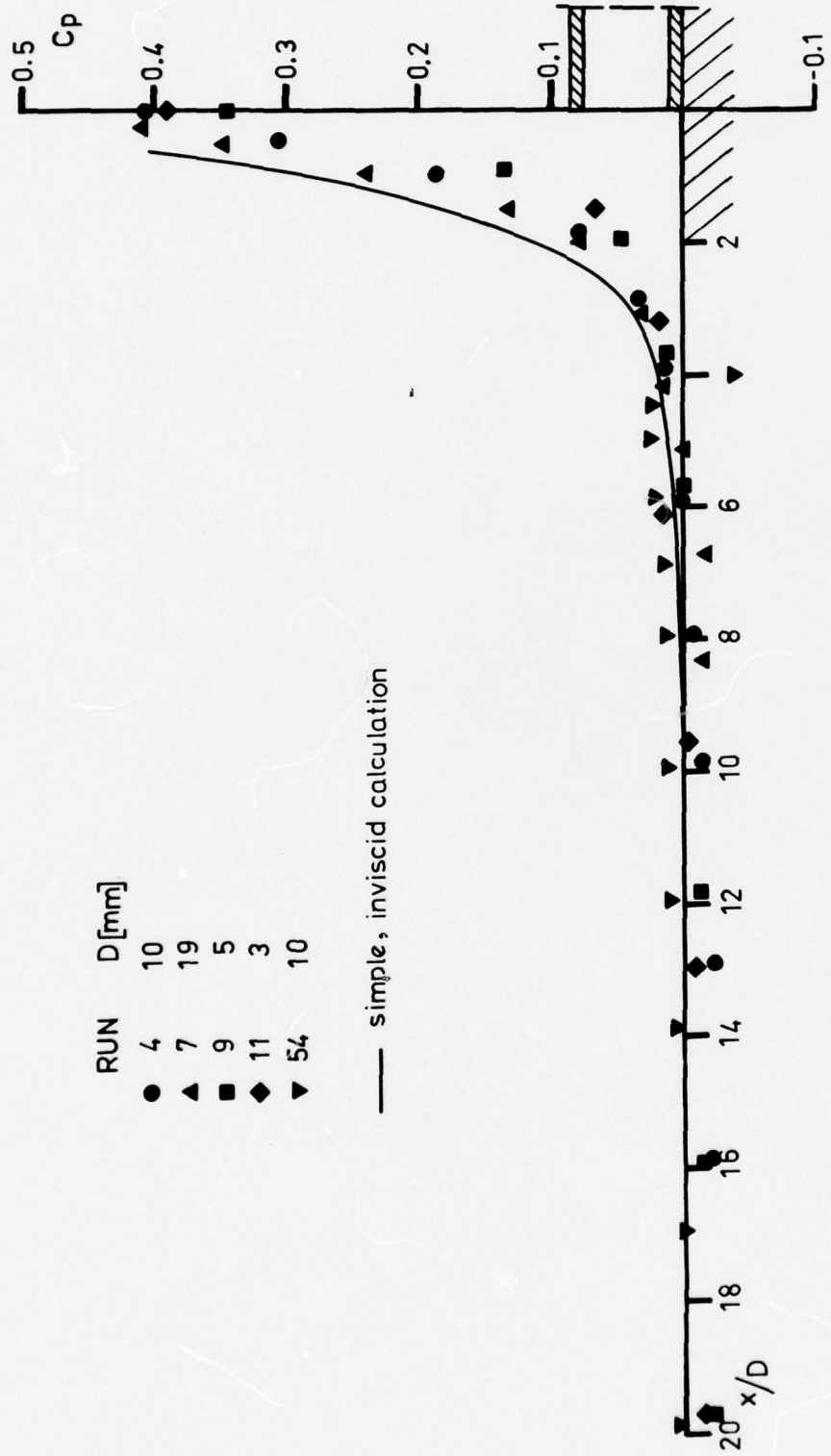

Figure 19. Measured pressure distribution along the cylinder centreline at $U_e \sim 20$ m/s for different diameters.

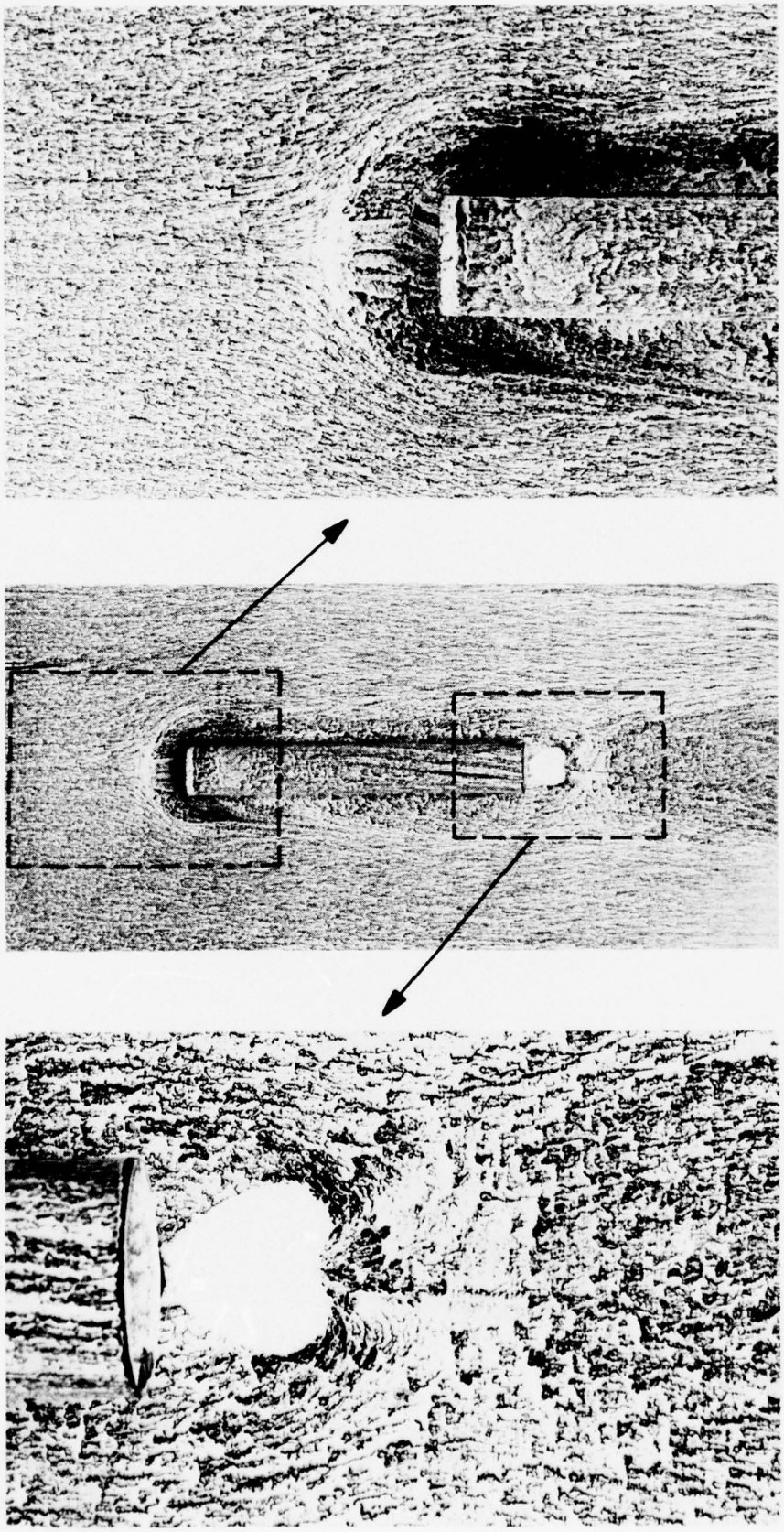

Figure 20. Surface flow visualization of the 19 mm cylinder. $U_e \sim 20$ m/s.

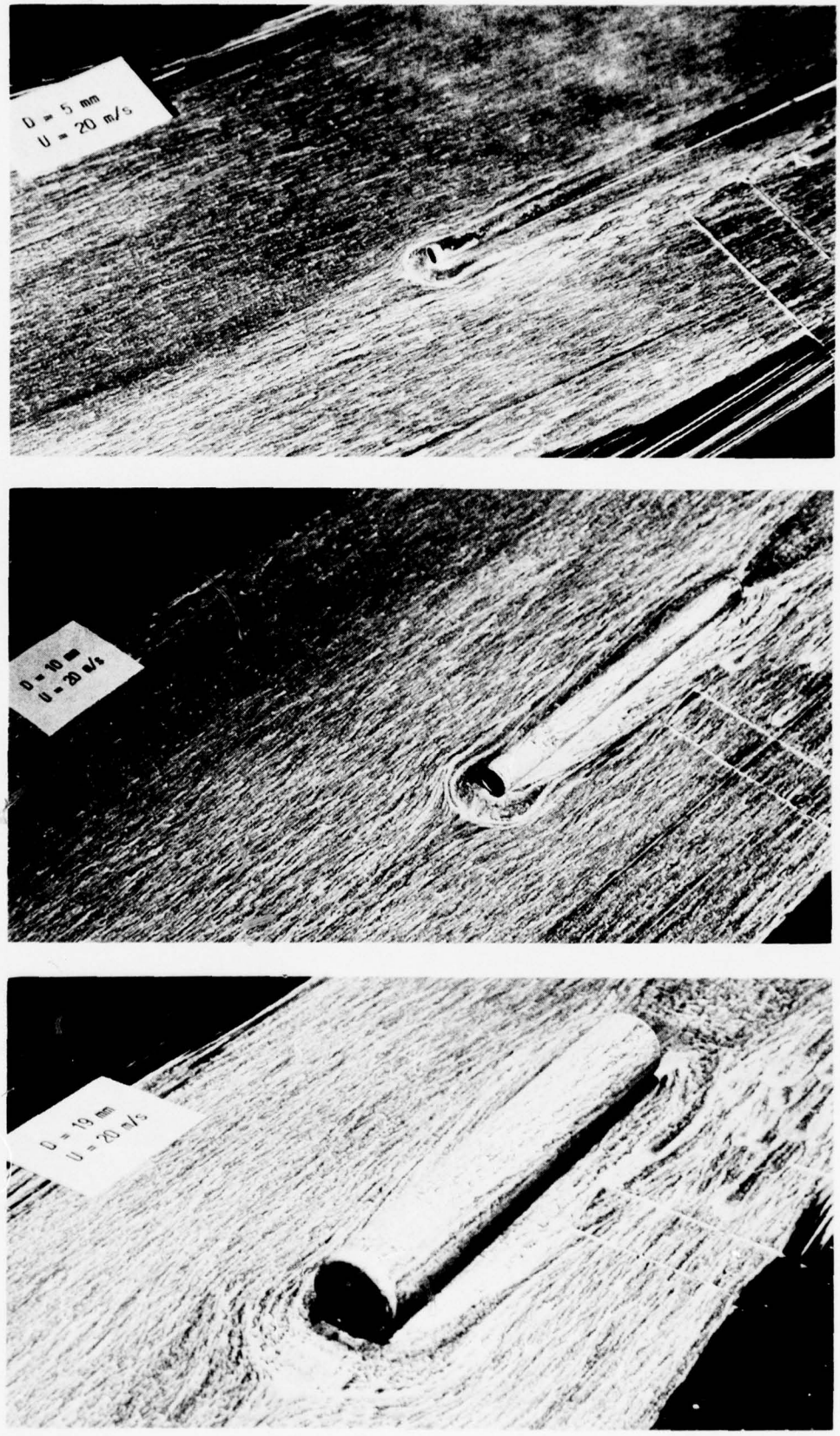

Figure 21. Surface flow visualization for cylinders of different diameters. $U_e \sim 20$ m/s.

D= 5 mm

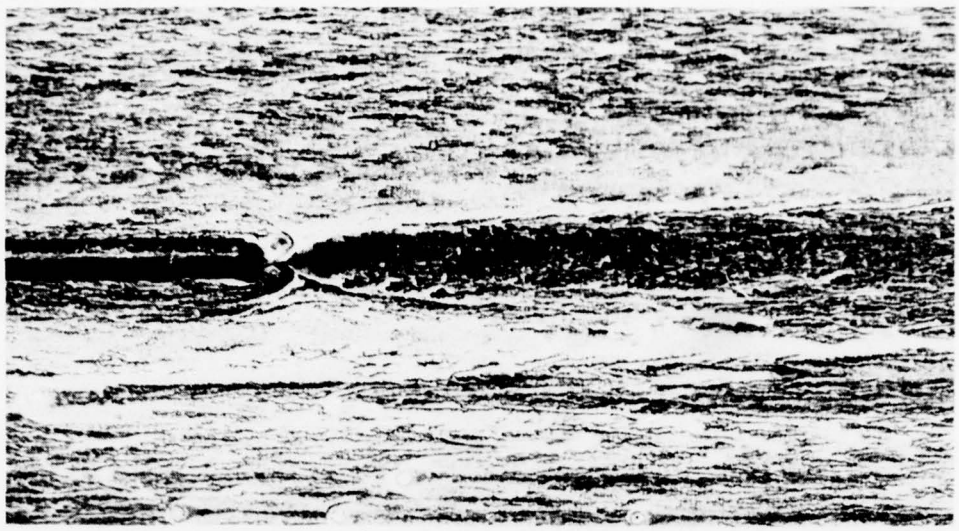

D= 10 mm

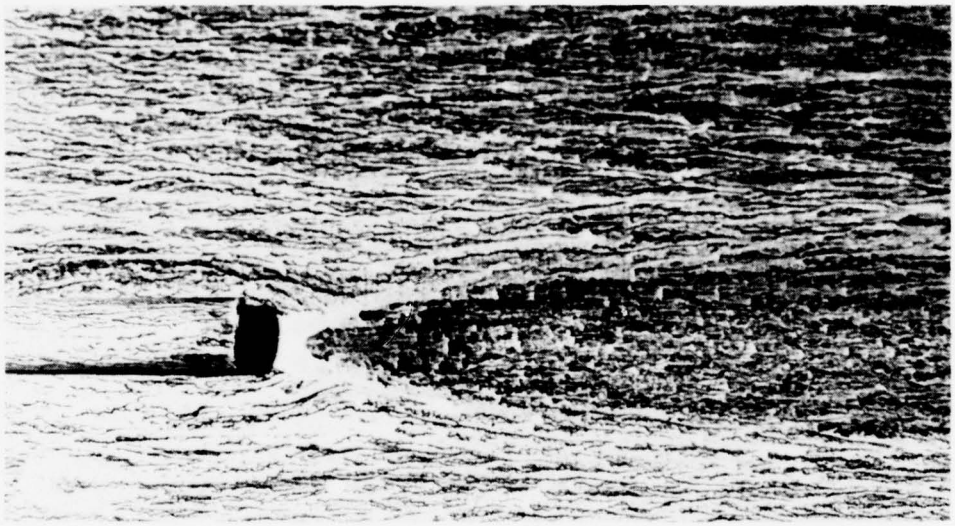

D= 19 mm

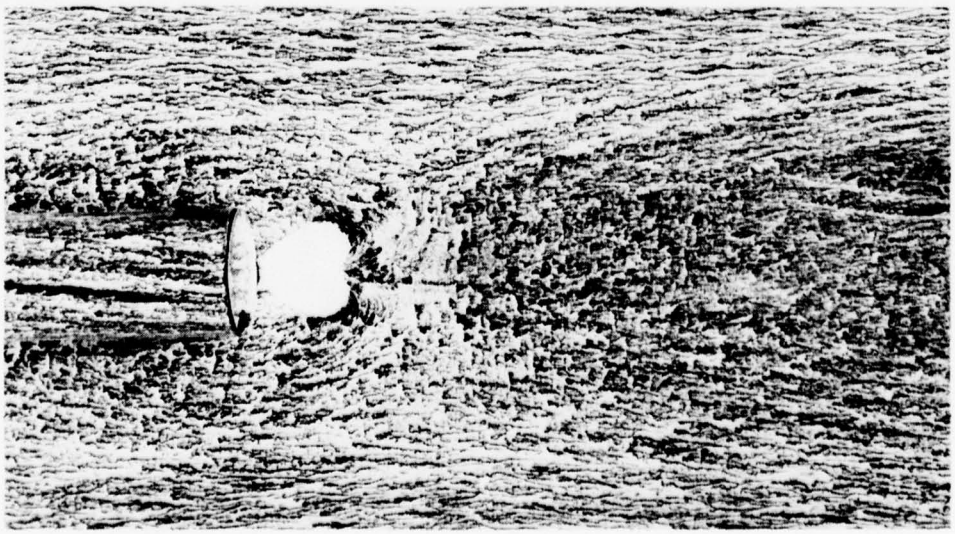

Figure 22. Surface flow visualization of wakes behind cylinders of different diameters. $U_e \sim 20$ m/s.

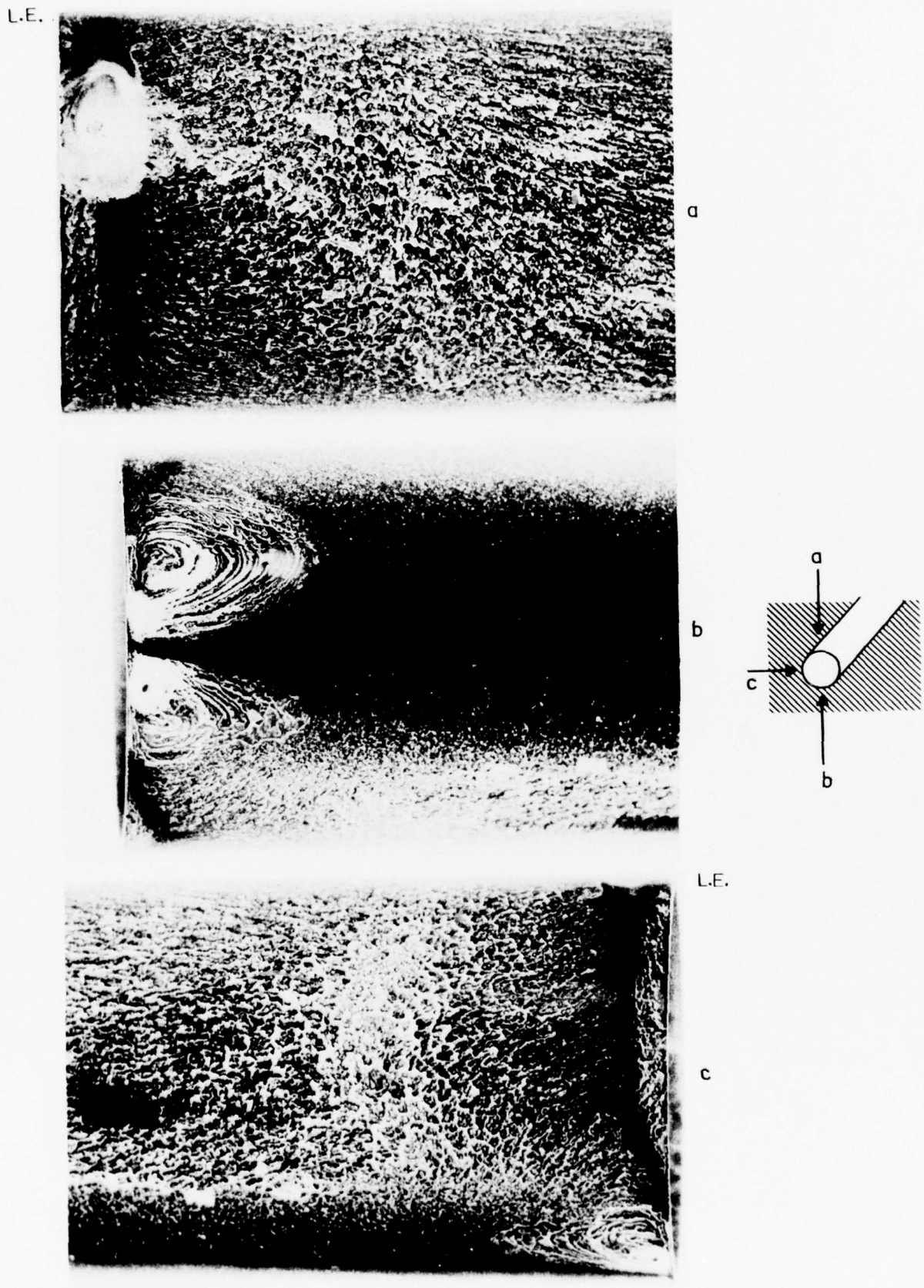

Figure 23. Surface flow pattern on the cylinder. Three different views. D= 19 mm.

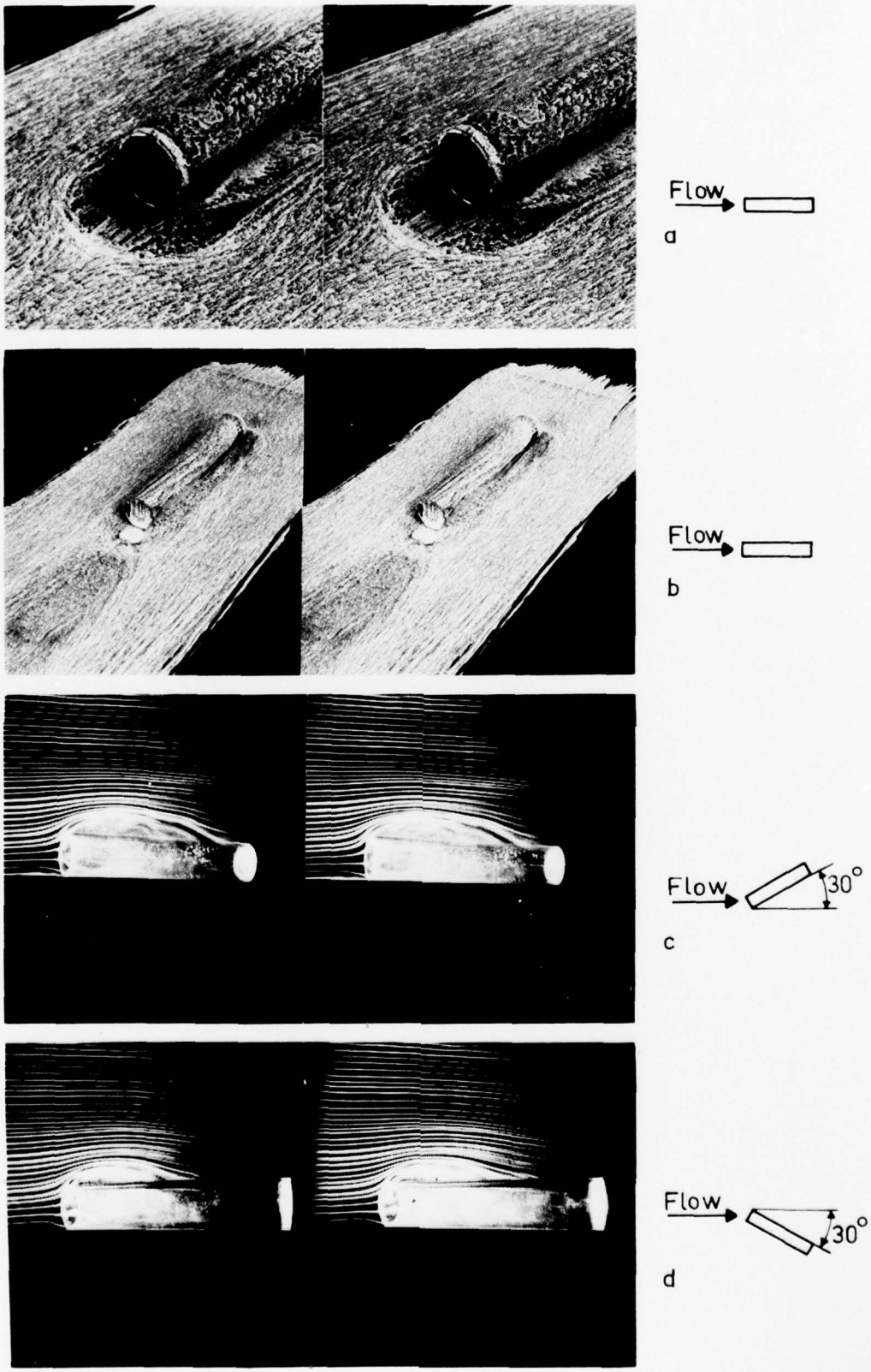

Figure 24. Stereo pictures of oil flows (a & b) and smoke visualizations (c & d). Oil flows were taken at $U_e \sim 20$ m/s, $\delta \sim 50$ mm, D= 19 mm. The smoke pictures are taken in potential flow; $U_e \sim 2$ m/s. Lenses should be used.

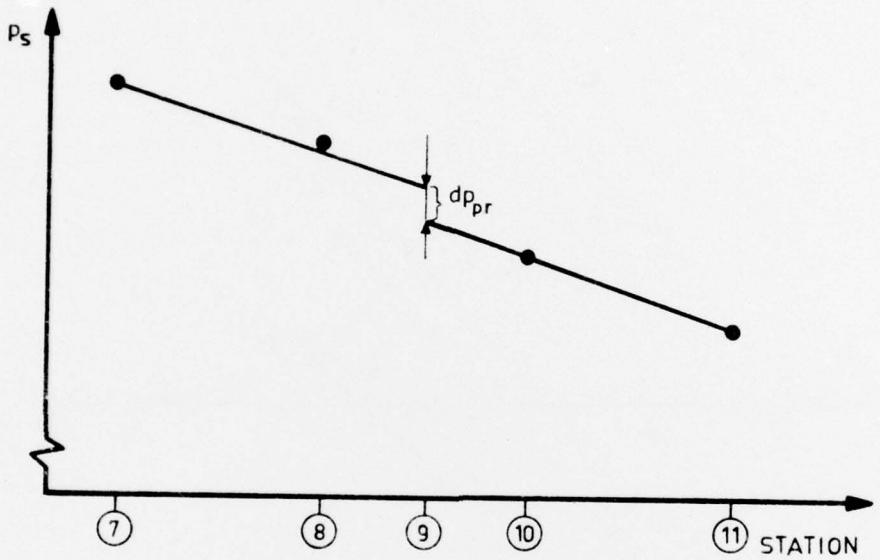

Figure 25. Deduction of pressure drop dp_{pr} due to the presence of the Preston tube.

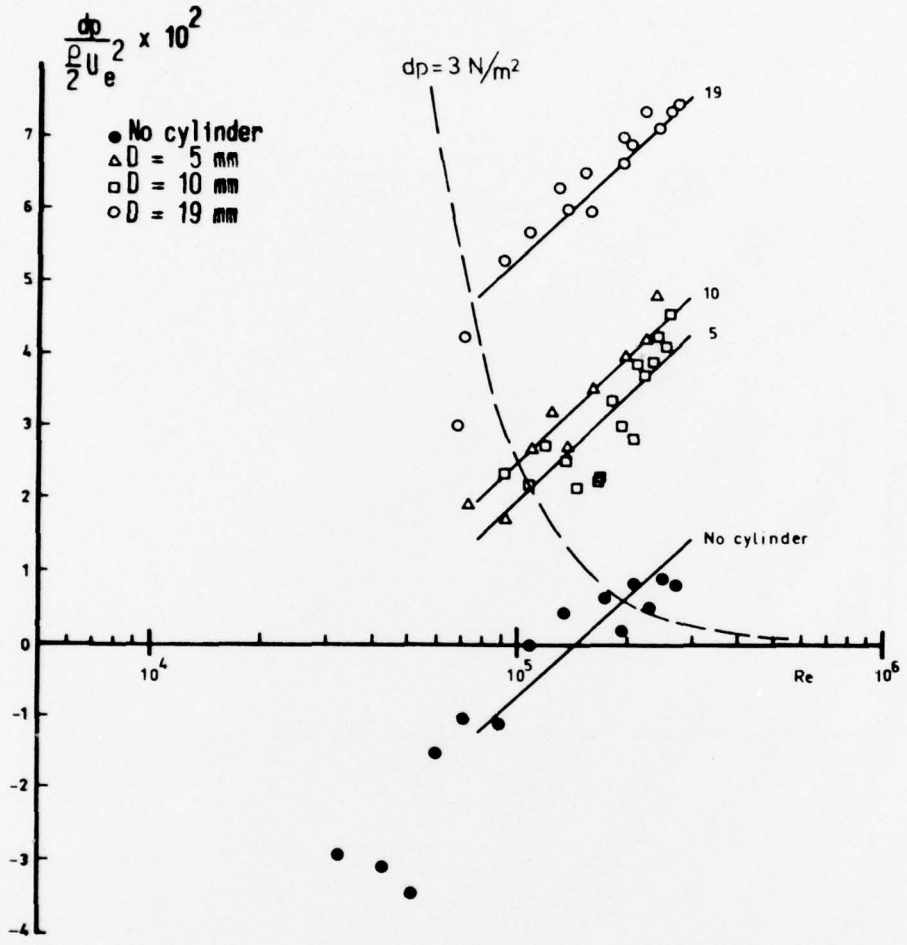

Figure 26. Pressure drop due to the presence of the cylinder. A line corresponding to dp= 3 N/m^2 is also plotted.

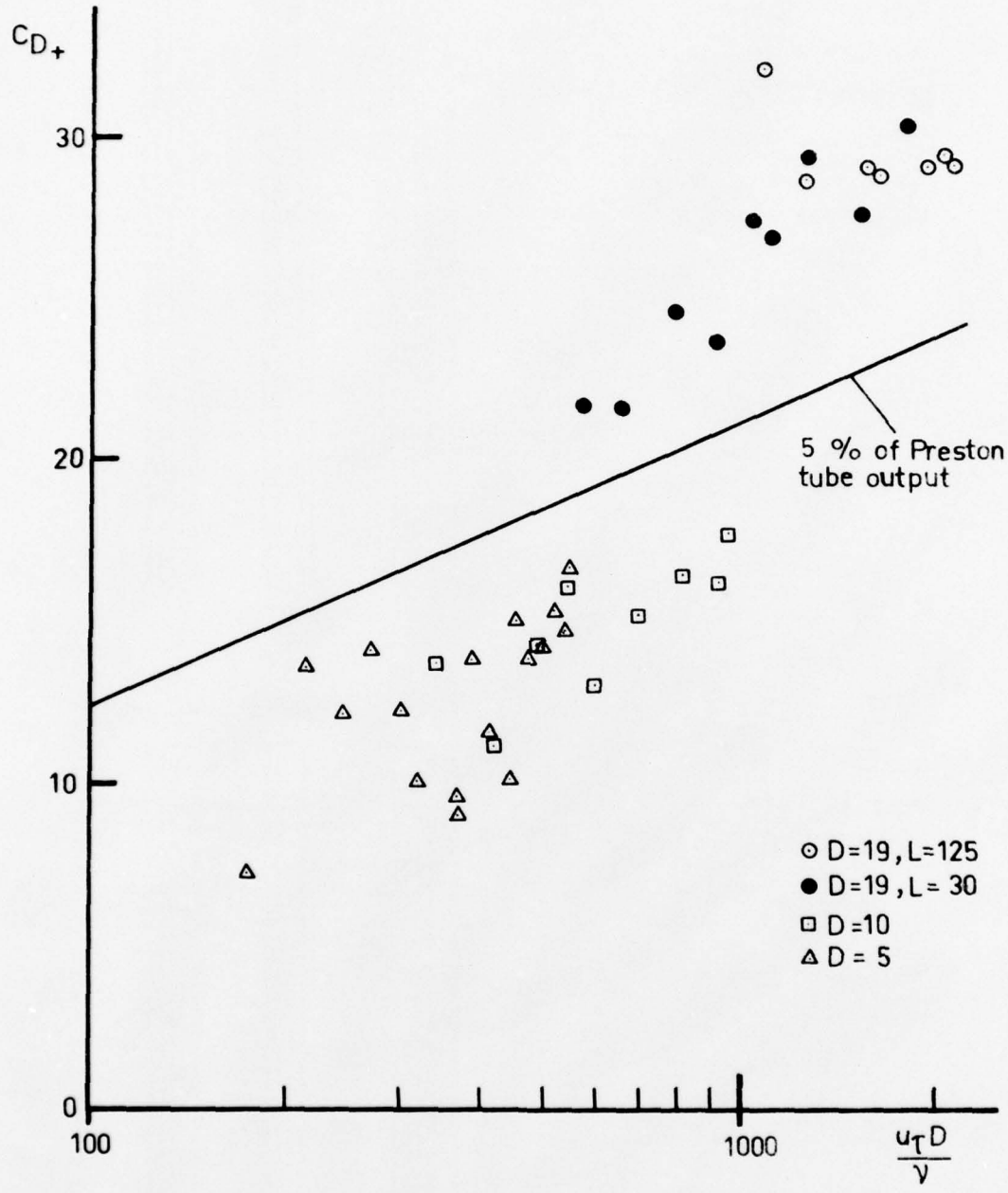

Figure 27. Cylinder drag coefficient C_{D_+} versus $u_\tau D/\nu$ for different tubes.

Table 1.

Run 310
Profile 16
Cylinder: D = 19
X = 151

$Re = 1.11 \cdot 10^5$
R+ = 5140

y [m]	U [m/s]	$\sqrt{u'^2}$ [m/s] *)
0.00149	1.97	0.760
0.00159	2.00	0.774
0.00179	2.11	0.853
0.00209	2.25	0.920
0.00309	2.61	1.062
0.00409	2.76	1.158
0.00509	2.97	1.171
0.00609	3.23	1.255
0.00709	3.26	1.284
0.00809	3.36	1.299
0.00909	3.36	1.329
0.01009	3.40	1.345
0.01109	3.43	1.416
0.01209	3.62	1.500
0.01309	3.90	1.793
0.01409	4.62	1.955
0.01509	5.34	2.082
0.01609	6.27	2.310
0.01709	7.35	2.447
0.01809	8.78	2.533
0.01909	10.64	2.504
0.02109	13.80	2.023
0.02309	15.66	1.589
0.02509	16.52	1.416
0.02809	17.24	1.240
0.03209	18.03	1.038
0.03709	18.75	0.858
0.04209	19.18	0.787
0.04709	19.53	0.702
0.05235	19.82	0.622
0.04776	19.89	0.597
0.04276	19.82	0.633
0.03776	19.53	0.702
0.03276	19.18	0.796
0.02776	18.67	0.888
0.02276	18.10	0.974
0.01776	17.46	1.062
0.01276	16.88	1.171
0.00976	16.45	1.248
0.00776	16.31	1.322
0.00576	16.24	1.408
0.00476	16.02	1.432
0.00376	15.30	1.457

Run 311
Profile 17
Cylinder: D = 19
X = 151

$Re = 5.99 \cdot 10^4$
R+ = 3100

y [m]	U [m/s]	$\sqrt{u'^2}$ [m/s]
0.00376	7.70	0.710
0.00476	8.06	0.698
0.00576	8.21	0.670
0.00776	8.49	0.651
0.00976	8.64	0.633
0.01276	8.99	0.615
0.01776	9.50	0.574
0.02276	9.93	0.532
0.02776	10.21	0.497
0.03276	10.43	0.448
0.03776	10.57	0.397
0.04276	10.79	0.350
0.04776	10.79	0.332
0.05235	10.72	0.336
0.04709	10.57	0.377
0.04209	10.50	0.438
0.03709	10.21	0.474
0.03309	9.93	0.535
0.03009	9.85	0.625
0.02809	9.14	0.655
0.02709	9.07	0.710
0.02609	9.21	0.774
0.02409	8.78	0.824
0.02309	8.64	0.920
0.02209	7.99	1.032
0.02109	7.65	1.240
0.02009	6.56	1.408
0.01909	5.48	1.432
0.01809	4.69	1.424
0.01709	3.76	1.284
0.01609	3.19	1.262
0.01509	2.68	1.068
0.01409	2.25	0.899
0.01309	2.04	0.783
0.01209	1.97	0.674
0.01109	1.90	0.651
0.01009	1.82	0.594
0.00909	1.82	0.590
0.00809	1.82	0.587
0.00709	1.82	0.587
0.00609	1.75	0.567
0.00509	1.68	0.541
0.00409	1.61	0.517
0.00309	1.61	0.480
0.00209	1.47	0.388
0.00179	1.39	0.348
0.00159	1.32	0.298
0.00139	1.25	0.275
0.00109	1.18	0.236

*) $\sqrt{u'^2}$ = RMS

Run 313
Profile 18
Cylinder: D = 10
X = 151

Re = $1.16 \cdot 10^5$
R+ = 5280

y [m]	U [m/s]	$\sqrt{u'^2}$ [m/s]
0.00079	3.83	0.690
0.00109	6.20	1.125
0.00159	6.99	1.158
0.00209	7.27	1.185
0.00259	7.42	1.212
0.00309	7.62	1.240
0.00409	7.78	1.392
0.00509	7.99	1.535
0.00609	9.14	1.654
0.00709	9.64	1.732
0.00809	10.21	1.814
0.00909	10.79	1.921
0.01009	11.50	2.023
0.01109	12.44	2.047
0.01209	13.51	1.943
0.01309	14.44	1.732
0.01409	15.09	1.607
0.01509	15.66	1.466
0.01609	16.09	1.376
0.01709	16.24	1.337
0.01909	16.81	1.248
0.02109	17.17	1.171
0.02309	17.38	1.125
0.02509	17.74	1.087
0.02809	18.03	1.044
0.03109	18.24	0.997
0.03709	18.82	0.909
0.04209	19.25	0.820
0.04709	19.68	0.726
0.05235	19.89	0.651
0.04776	19.89	0.636
0.04276	19.75	0.674
0.03776	19.39	0.769
0.03276	19.10	0.848
0.02776	18.53	0.941
0.02276	17.96	1.032
0.01776	17.31	1.125
0.01276	16.59	1.233
0.00976	15.95	1.299
0.00776	15.73	1.376
0.00676	15.59	1.408
0.00576	15.52	1.449
0.00476	15.23	1.483
0.00376	14.73	1.491
0.00326	14.23	1.491
0.00276	13.80	1.500
0.00226	13.08	1.509
0.00176	12.51	1.544
0.05235	19.68	0.651

Run 314
Profile 19
Cylinder: D = 10
X = 151

Re = $6.30 \cdot 10^4$
R+ = 3130

y [m]	U [m/s]	$\sqrt{u'^2}$ [m/s]
0.00176	6.70	0.815
0.00276	7.27	0.760
0.00376	7.63	0.752
0.00476	8.06	0.747
0.00576	8.35	0.747
0.00776	8.49	0.714
0.00976	8.56	0.686
0.01276	8.99	0.647
0.01776	9.07	0.587
0.02276	9.50	0.548
0.02776	9.85	0.508
0.03276	10.00	0.453
0.03776	10.36	0.411
0.04276	10.50	0.368
0.04776	10.79	0.346
0.05235	10.57	0.332
0.05235	10.79	0.348
0.05249	10.72	0.338
0.04709	10.64	0.377
0.04209	10.50	0.416
0.03709	10.21	0.461
0.03209	9.93	0.511
0.02709	9.64	0.545
0.02209	9.35	0.594
0.01909	8.99	0.659
0.01809	8.92	0.682
0.01709	8.78	0.702
0.01609	8.64	0.730
0.01509	8.35	0.774
0.01409	8.06	0.843
0.01309	7.85	0.920
0.01259	7.42	0.965
0.01209	7.27	1.014
0.01159	7.06	1.050
0.01109	6.77	1.062
0.01059	6.49	1.068
0.01009	6.20	1.050
0.00959	6.05	1.025
0.00909	5.91	0.991
0.00859	5.77	0.946
0.00809	5.62	0.925
0.00759	5.48	0.893
0.00709	5.27	0.868
0.00609	4.98	0.843
0.00509	4.41	0.815
0.00409	4.19	0.774
0.00309	3.90	0.730
0.00259	3.83	0.702
0.00209	3.69	0.670
0.00159	3.47	0.618
0.00109	2.60	0.532
0.00109	2.90	0.532
0.00099	2.68	0.483
0.00089	2.25	0.411
0.00084	1.97	0.326
0.00079	1.47	0.206
0.00074	1.39	0.072
0.00069	0.89	0.162
0.00069	1.54	0.051
0.00064	1.61	0.065
0.00059	1.47	0.055

Run 315
Profile 20
Cylinder: D = 5
X = 151

Re = $1.20 \cdot 10^5$
R+ = 5650

y [m]	U [m/s]	$\sqrt{u'^2}$ [m/s]
0.00079	3.19	0.246
0.00089	5.84	0.765
0.00094	3.19	0.366
0.00099	3.04	0.342
0.00109	6.27	0.878
0.00109	4.33	0.580
0.00119	7.13	0.980
0.00129	7.78	0.946
0.00159	9.07	0.941
0.00209	10.00	1.002
0.00259	10.43	1.093
0.00309	10.79	1.178
0.00409	11.50	1.198
0.00509	11.65	1.158
0.00709	11.72	1.164
0.00809	11.79	1.314
0.00909	12.51	1.783
0.01009	13.44	1.921
0.01109	14.37	1.814
0.01209	14.80	1.589
0.01309	15.45	1.416
0.01409	15.81	1.262
0.01509	15.95	1.226
0.01709	16.16	1.164
0.01909	16.52	1.125
0.02209	16.95	1.093
0.02709	17.53	1.038
0.03209	18.24	0.985
0.03709	18.89	0.899
0.04209	19.53	0.810
0.04709	19.96	0.718
0.05235	19.68	0.615
0.05235	20.18	0.651
0.04776	20.18	0.608
0.04276	19.75	0.644
0.03776	19.39	0.722
0.03276	19.03	0.810
0.02776	18.53	0.899
0.02276	17.81	0.985
0.01776	17.24	1.062
0.01276	16.45	1.138
0.00976	15.95	1.212
0.00776	15.45	1.262
0.00676	15.23	1.269
0.00576	15.23	1.314
0.00476	15.02	1.337
0.00376	14.59	1.360
0.00276	14.01	1.376
0.00176	13.15	1.392
0.00076	12.01	1.400

Run 316
Profile 21
Cylinder: D = 19
X = 182

Re = $1.14 \cdot 10^5$
R+ = 5760

y [m]	U [m/s]	$\sqrt{u'^2}$ [m/s]
0.00176	10.88	1.486
0.00376	13.69	1.363
0.00576	15.49	1.363
0.00776	15.94	1.317
0.00976	16.19	1.243
0.00976	16.26	1.265
0.01276	16.77	1.194
0.01776	17.67	1.121
0.02276	18.43	1.005
0.02776	19.01	0.932
0.03276	19.52	0.841
0.03776	20.04	0.749
0.04276	20.36	0.656
0.04776	20.55	0.616
0.05235	20.68	0.634
0.04709	20.55	0.711
0.04209	20.16	0.817
0.03709	19.65	0.922
0.03209	19.01	1.034
0.02709	18.24	1.265
0.02409	17.22	1.716
0.02209	16.51	2.186
0.02009	14.27	2.598
0.01809	12.48	2.881
0.01709	11.64	2.832
0.01509	10.17	2.628
0.01309	9.08	2.424
0.01109	8.44	2.198
0.01009	8.19	2.112
0.00809	7.80	2.005
0.00609	7.48	1.948
0.00409	7.16	1.926
0.00209	6.65	1.839

Run 317
Profile 22
Cylinder: D = 19
X = 31

Re = $1.12 \cdot 10^5$
R+ = 5590

y [m]	U [m/s]	$\sqrt{u'^2}$ [m/s]
0.00176	9.79	1.504
0.00276	12.22	1.379
0.00376	13.69	1.325
0.00576	15.17	1.317
0.00776	16.13	1.302
0.00976	16.38	1.243
0.01276	16.96	1.194
0.01776	17.86	1.089
0.02276	18.56	1.005
0.02776	19.20	0.927
0.03276	19.72	0.831
0.03776	20.10	0.745
0.04276	20.55	0.653
0.04776	20.74	0.602
0.05235	20.68	0.630
0.04709	20.42	0.699
0.04209	20.23	0.817
0.03709	19.52	0.927
0.03309	19.20	0.993
0.03009	18.88	1.058
0.02809	18.63	1.108
0.02609	18.31	1.236
0.02509	17.99	1.395
0.02409	17.73	1.707
0.02309	17.09	2.064
0.02259	16.58	2.263
0.02209	16.00	2.424
0.02159	15.42	2.524
0.02109	14.78	2.658
0.02059	14.01	2.705

Run 318
Profile 23
Cylinder: D = 19
X = 0.5

Re = $1.11 \cdot 10^5$
R+ = 5590

y [m]	U [m/s]	$\sqrt{u'^2}$ [m/s]
0.00176	10.04	1.639
0.00276	12.03	1.583
0.00376	13.89	1.419
0.00576	15.42	1.332
0.00776	16.13	1.272
0.00976	16.06	1.229
0.01276	16.58	1.147
0.01776	17.47	1.052
0.02276	17.99	0.965
0.02776	18.63	0.870
0.03276	19.07	0.776
0.03776	19.52	0.691
0.04276	19.97	0.616
0.04776	20.16	0.572
0.05235	20.23	0.588
0.04709	20.04	1.181
0.04209	19.65	0.758
0.03709	19.27	0.855
0.03309	18.82	0.911
0.03009	18.63	0.949
0.02809	18.43	0.976
0.02609	18.18	1.028
0.02409	17.99	1.046
0.02309	17.92	1.071
0.02259	17.86	1.089
0.02209	17.73	1.096
0.02159	17.67	1.108
0.02109	17.60	1.128
0.02059	17.47	1.141

Run 319

Profile 24

Cylinder: D = 19

X = 3.5

Re = $1.14 \cdot 10^5$

R+ = 5750

y [m]	U[m/s]	$\sqrt{u'^2}$ [m/s]
0.00176	9.27	1.948
0.00276	11.58	1.495
0.00376	13.57	1.387
0.00576	15.42	1.325
0.00776	16.38	1.302
0.00976	16.38	1.236
0.01276	16.90	1.174
0.01776	17.67	1.077
0.02276	18.37	0.982
0.02776	19.01	0.896
0.03276	19.52	0.803
0.03776	20.04	0.716
0.04276	20.29	0.630
0.04776	20.55	0.592
0.05235	20.48	0.599
0.04709	20.23	0.687
0.04209	19.91	0.776
0.03709	19.52	0.850
0.03209	18.95	0.943
0.03009	18.88	0.965
0.02809	18.75	0.999
0.02609	18.69	1.017
0.02409	18.69	1.046
0.02309	18.69	1.071
0.02209	18.88	1.083
0.02159	19.01	1.121
0.02109	19.14	1.147
0.02059	19.39	1.181
0.02009	19.52	1.229

Run 320

Profile 25

Cylinder: D = 19

X = -27

Re = $1.16 \cdot 10^5$

R+ = 6010

y [m]	U[m/s]	$\sqrt{u'^2}$ [m/s]
0.00176	10.56	2.064
0.00376	13.69	1.419
0.00576	15.10	1.348
0.00776	15.94	1.325
0.00976	16.13	1.251
0.01276	16.58	1.194
0.01776	17.60	1.096
0.02276	18.11	1.005
0.02776	18.75	0.916
0.03276	19.20	0.822
0.03776	19.59	0.741
0.04276	20.04	0.645
0.04776	20.10	0.599
0.05235	20.04	0.602
0.04709	19.78	0.672
0.04209	19.39	0.767
0.03709	18.75	0.865
0.03209	18.11	0.949
0.02709	17.35	1.022
0.02409	16.70	1.071
0.02109	16.13	1.128
0.01909	15.81	1.194
0.01709	15.42	1.229
0.01509	14.78	1.243
0.01409	14.65	1.251
0.01309	14.40	1.265
0.01209	14.21	1.287
0.01109	13.89	1.317
0.01009	13.76	1.332
0.00909	13.37	1.411
0.00809	12.99	1.444
0.00709	12.54	1.547
0.00609	11.96	1.611
0.00509	11.45	1.658
0.00409	10.68	1.658
0.00309	9.91	1.639
0.00259	9.66	1.639
0.00209	9.27	1.620
0.00159	8.89	1.593

Run 321
Profile 26
Cylinder: D = 19
X = -19.5

Re = $1.16 \cdot 10^5$
R+ = 6040

y [m]	U [m/s]	$\sqrt{u'^2}$ [m/s]
0.00176	9.72	1.668
0.00376	13.76	1.403
0.00576	15.42	1.403
0.00776	16.26	1.387
0.00976	16.45	1.302
0.01276	17.22	1.229
0.01776	17.99	1.134
0.02276	18.75	1.058
0.02776	19.46	0.960
0.03276	19.91	0.870
0.03776	20.16	0.780
0.04276	20.55	0.675
0.04776	20.74	0.627
0.05235	20.68	0.634
0.04709	20.42	0.699
0.04209	20.04	0.798
0.03709	19.33	0.896
0.03209	18.75	0.976
0.02709	17.86	1.071
0.02409	17.22	1.108
0.02109	16.58	1.160
0.01909	16.13	1.187
0.01709	15.62	1.229
0.01509	15.10	1.251
0.01409	14.65	1.287
0.01309	14.21	1.302
0.01209	13.95	1.340
0.01109	13.63	1.356
0.01009	13.25	1.379
0.00909	12.80	1.444
0.00809	12.41	1.4[illegible]
0.00709	11.96	1.5[illegible]7
0.00609	11.45	1.574
0.00509	10.81	1.593
0.00409	10.62	1.620
0.00309	9.98	1.639
0.00209	8.89	1.668
0.00159	8.31	1.697

Run 322
Profile 27
Cylinder: D = 19
X = -19.5

Re = $5.89 \cdot 10^5$
R+ = 3360

y [m]	U [m/s]	$\sqrt{u'^2}$ [m/s]
0.00176	4.21	0.785
0.00376	6.97	0.653
0.00576	7.80	0.660
0.00776	8.12	0.653
0.00976	8.57	0.599
0.01776	9.15	0.555
0.02276	9.40	0.518
0.02776	9.79	0.478
0.03276	10.04	0.429
0.03776	10.30	0.380
0.04276	10.43	0.341
0.04776	10.49	0.309
0.05235	10.49	0.305
0.04709	10.36	0.327
0.04209	10.24	0.367
0.03709	9.85	0.412
0.03209	9.53	0.449
0.02709	9.15	0.495
0.02409	8.76	0.509
0.02109	8.51	0.533
0.01909	8.31	0.549
0.01709	8.12	0.575
0.01509	7.80	0.599
0.01409	7.61	0.616
0.01309	7.48	0.623
0.01209	7.03	0.602
0.01109	6.97	0.630
0.01009	6.84	0.645
0.00909	6.58	0.668
0.00709	6.07	0.703
0.00509	5.62	0.732
0.00309	5.11	0.749
0.00209	4.73	0.789

Run 323

Profile 28

Cylinder: D = 19

X = -3.5

Re = $1.24 \cdot 10^5$

R+ = 6290

y [m]	U [m/s]	$\sqrt{u'^2}$ [m/s]
0.00176	8.53	1.778
0.00376	14.00	1.505
0.00576	16.16	1.454
0.00776	16.90	1.412
0.00976	17.38	1.357
0.01276	18.32	1.295
0.01776	19.40	1.195
0.02276	20.21	1.115
0.02776	20.89	1.000
0.03276	21.49	0.917
0.03776	22.17	0.803
0.04276	22.44	0.724
0.04776	22.51	0.668
0.05235	22.17	0.668
0.04709	21.83	0.750
0.04209	21.43	0.846
0.03709	20.82	0.949
0.03209	20.21	1.029
0.02709	19.47	1.115
0.02409	18.79	1.188
0.02209	18.19	1.295
0.02009	17.11	1.412
0.01909	16.50	1.479
0.01809	15.76	1.585
0.01709	14.95	1.748
0.01609	14.27	1.873
0.01509	13.66	2.053
0.01409	13.19	2.213
0.01309	12.65	2.357
0.01209	11.71	2.412
0.01109	10.56	2.511
0.01009	9.48	2.526
0.00909	8.53	2.585
0.00809	7.66	2.615
0.00709	7.12	2.615
0.00609	6.91	2.707
0.00509	7.12	2.834
0.00409	7.32	2.985
0.00309	7.39	2.968
0.00259	7.32	2.770
0.00209	6.98	2.630
0.00159	6.51	2.371

Run 324

Profile 29

Cylinder: D = 19

X = -8.5

Re = $6.96 \cdot 10^3$

R+ = 460 *

y [m]	U [m/s]	$\sqrt{u'^2}$ [m/s]
0.00776	1.28	0.022
0.01276	1.43	0.022
0.02776	1.66	0.022
0.04276	1.66	0.022
0.05235	1.65	0.022
0.05235	1.65	0.022
0.04209	1.58	0.022
0.03209	1.51	0.022
0.02209	1.44	0.022
0.01709	1.31	0.022
0.01209	1.17	0.022
0.00709	0.97	0.022
0.00709	0.97	0.027
0.00509	0.99	0.917
0.00409	0.90	0.043
0.00309	1.07	0.052
0.00209	1.11	0.055

*) Based on calculated f

Run 325
Profile 30
Cylinder: D = 19
X = -8.5

Re = $1.23 \cdot 10^4$
R+ = 740 *

y [m]	U [m/s]	$\sqrt{u'^2}$ [m/s]
0.00776	1.58	0.022
0.01276	1.93	0.022
0.01776	2.12	0.022
0.02776	2.23	0.022
0.03776	2.23	0.022
0.05235	2.39	0.022
0.04209	2.39	0.022
0.03209	2.39	0.022
0.02209	2.25	0.022
0.01709	2.09	0.046
0.01209	1.85	0.077
0.00909	1.31	0.150
0.00509	1.11	0.106
0.00409	1.15	0.112
0.00309	1.17	0.145
0.00209	1.20	0.150

Run 326
Profile 31
Cylinder: D = 19
X = -8.5

Re = $1.30 \cdot 10^5$
R+ = 5970 *

y [m]	U [m/s]	$\sqrt{u'^2}$ [m/s]
0.00776	16.84	1.420
0.00976	17.51	1.404
0.01276	18.19	1.341
0.01776	19.13	1.223
0.02276	19.54	1.155
0.02776	20.41	1.017
0.03276	21.16	0.917
0.03776	21.36	0.799
0.04276	21.90	0.708
0.04776	22.10	0.688
0.05235	22.17	0.720
0.04709	21.97	0.827
0.04209	21.49	0.944
0.03709	20.75	1.041
0.03209	20.21	1.135
0.02709	19.20	1.223
0.02409	18.46	1.281
0.02109	17.38	1.412
0.01709	15.62	1.640
0.01409	14.41	1.851
0.01209	13.39	2.113
0.01009	11.98	2.226
0.00809	10.22	2.304
0.00709	10.09	2.317
0.00609	8.47	2.497
0.00509	7.79	2.511
0.00409	7.12	2.585
0.00309	6.30	2.660
0.00259	6.10	2.834
0.00209	6.14	0.516

Run 332
Profile 37
Cylinder: D = 19
X = 11.5

Re = $1.24 \cdot 10^5$
R+ = 5740 *

y [m]	U [m/s]	$\sqrt{u'^2}$ [m/s]
0.00776	15.96	1.288
0.00976	16.16	1.223
0.01276	16.77	1.161
0.01776	17.58	1.059
0.02276	18.32	0.977
0.02776	19.06	0.891
0.03276	19.40	0.794
0.03776	20.01	0.688
0.04276	20.41	0.620
0.04776	20.48	0.592
0.05235	20.48	0.627
0.04709	20.28	0.716
0.04209	19.94	0.817
0.03709	19.54	0.917
0.03409	19.20	0.960
0.03109	19.00	0.983
0.02909	18.86	1.017
0.02709	18.79	1.071
0.02509	18.66	1.128
0.02309	18.12	1.437
0.02209	18.59	1.961

*) Based on calculated f

Run 333
Profile 38
Cylinder: D = 19
X = -16

Re = $1.29 \cdot 10^5$
R+ = 5960 *

y [m]	U [m/s]	$\sqrt{u'^2}$ [m/s]
0.00776	16.16	1.357
0.00976	16.84	1.295
0.01276	17.44	1.223
0.01776	18.39	1.122
0.02276	19.13	1.029
0.02776	19.81	0.960
0.03276	20.28	0.851
0.03776	20.75	0.750
0.04276	21.02	0.664
0.04776	20.95	0.635
0.05235	21.02	0.664
0.04709	20.75	0.781
0.04209	20.21	0.876
0.03709	19.54	0.966
0.03209	18.86	1.041
0.02709	17.85	1.109
0.02209	16.77	1.209
0.01909	16.03	1.244
0.01709	15.42	1.281
0.01509	14.81	1.318
0.01309	14.00	1.364
0.01109	13.06	1.462
0.01009	12.52	1.496
0.00909	11.98	1.576
0.00809	11.23	1.659
0.00709	10.63	1.728
0.00609	9.88	1.851
0.00509	9.01	1.950
0.00409	8.33	2.006
0.00309	7.39	2.089
0.00259	6.84	2.101
0.00209	6.30	2.113
0.00159	5.63	2.065

Run 334
Profile 39
Cylinder: D = 19
X = -11

Re = $1.26 \cdot 10^5$
R+ = 5840 *

y [m]	U [m/s]	$\sqrt{u'^2}$ [m/s]
0.00776	16.57	1.404
0.00976	16.84	1.266
0.01276	17.51	1.188
0.01776	18.39	1.090
0.02276	19.13	1.011
0.02776	19.81	0.922
0.03276	20.35	0.817
0.03776	20.75	0.720
0.04276	21.02	0.642
0.04776	21.16	0.613
0.05235	21.02	0.642
0.04709	20.82	0.729
0.04209	20.28	0.836
0.03709	19.60	0.928
0.03209	18.86	0.994
0.02709	17.92	1.065
0.02209	16.70	1.161
0.01909	15.76	1.259
0.01709	15.08	1.326
0.01509	14.41	1.388
0.01309	13.60	1.487
0.01109	12.52	1.612
0.01009	11.98	1.679
0.00909	11.30	1.728
0.00809	10.36	1.809
0.00709	9.68	1.862
0.00609	8.60	1.938
0.00509	7.72	2.053
0.00409	6.71	2.101
0.00359	6.17	2.113
0.00309	5.63	2.138
0.00259	5.22	2.101
0.00209	4.95	2.089
0.00159	4.82	2.077

Run 335
Profile 40
Cylinder: D = 19
X = 167

Re = $1.24 \cdot 10^5$
R+ = 5760 *

y [m]	U [m/s]	$\sqrt{u'^2}$ [m/s]
0.00776	16.57	1.326
0.00976	16.97	1.205
0.01276	17.44	1.216
0.01776	18.59	1.128
0.02276	19.40	1.029
0.02776	20.08	0.928
0.03276	20.62	0.851
0.03776	21.02	0.745
0.04276	21.29	0.661
0.04776	21.36	0.631
0.05235	21.29	0.664
0.04709	21.02	0.776
0.04209	20.48	0.881
0.03709	20.01	0.994
0.03409	19.60	1.059
0.03209	19.13	1.135
0.02909	18.79	1.216
0.02809	18.32	1.326
0.02709	18.12	1.372
0.02609	17.78	1.445
0.02509	17.65	1.470
0.02409	17.24	1.540
0.02309	16.36	1.631
0.02259	16.70	1.679
0.02209	16.50	1.738
0.02159	16.23	1.819
0.02109	15.82	1.905

*) Based on calculated f

Run 336
Profile 41
Cylinder: D = 19
X = 132.5

Re = $1.27 \cdot 10^5$
R+ = 5870 *

y [m]	U [m/s]	$\sqrt{u'^2}$ [m/s]
0.00776	16.30	1.223
0.00976	17.65	1.237
0.01276	18.32	1.168
0.01776	19.20	1.084
0.02276	20.08	1.000
0.02776	20.75	0.912
0.03276	21.36	0.827
0.03776	21.49	0.712
0.04276	21.97	0.631
0.04776	22.10	0.613
0.05235	22.03	0.657
0.04709	21.29	0.750
0.04209	20.55	0.841
0.03709	20.14	0.960
0.03209	19.67	1.103
0.02709	18.59	1.420
0.02209	16.84	1.612
0.02109	16.30	1.603
0.02009	12.92	2.150
0.01959	7.12	2.053
0.01909	3.06	1.096
0.01859	4.95	1.650
0.01809	2.25	0.772
0.01809	4.01	1.011
0.01709	2.32	0.794

Run 337
Profile 42
Cylinder: D = 19
X = 132.5

Re = $1.26 \cdot 10^5$
R+ = 5840 *

y [m]	U [m/s]	$\sqrt{u'^2}$ [m/s]
0.00776	16.16	1.281
0.00976	16.97	1.273
0.01276	17.71	1.209
0.01776	18.46	1.115
0.02276	19.13	1.029
0.02776	19.67	0.928
0.03276	20.28	0.832
0.03776	20.82	0.688
0.04276	21.02	0.646
0.04776	21.09	0.631
0.05235	20.95	0.672
0.04709	20.75	0.781
0.04209	20.21	0.891
0.03709	19.67	0.994
0.03209	19.13	1.148
0.02709	18.12	1.437
0.02409	17.38	1.576
0.02209	16.43	1.659
0.02109	15.42	1.679
0.02059	14.81	1.708
0.02039	13.93	1.830
0.02009	12.99	2.053
0.01979	9.68	2.277
0.01959	8.20	2.175
0.01949	6.78	2.053
0.01929	4.75	1.728
0.01909	3.74	1.462
0.01889	2.66	0.955
0.01869	2.28	0.733
0.01859	2.25	0.733
0.01849	2.25	0.708
0.01829	2.25	0.720
0.01809	2.25	0.750
0.01709	2.39	0.817
0.01609	2.46	0.846
0.01509	2.52	0.836
0.01409	2.66	0.841
0.01309	2.73	0.841
0.01209	2.66	0.841
0.01009	2.59	0.827
0.00809	2.39	0.794
0.00709	2.52	0.799
0.00509	2.56	0.817
0.00309	2.55	0.790
0.00209	2.50	0.745

Run 338
Profile 43
Cylinder: D = 19
X = 137.5

Re = $1.25 \cdot 10^5$
R+ = 5760 *

y [m]	U [m/s]	$\sqrt{u'^2}$ [m/s]
0.00776	16.16	1.295
0.01276	17.24	1.168
0.01776	18.12	1.071
0.02276	18.79	0.983
0.03276	19.81	0.803
0.04276	20.62	0.620
0.05235	20.62	0.631
0.05235	20.62	0.649
0.04776	20.64	0.599
0.04209	19.81	0.861
0.03709	19.33	0.955
0.03209	18.79	1.078
0.02709	17.85	1.333
0.02409	17.04	1.487
0.02209	16.30	1.576
0.02109	15.82	1.631
0.02009	14.81	1.873
0.01909	11.64	2.330
0.01859	9.34	2.412
0.01809	7.25	2.304
0.01759	5.29	2.030
0.01709	3.94	1.631
0.01659	3.13	1.266
0.01609	2.79	1.047
0.01509	2.86	1.053
0.01409	3.13	1.128
0.01309	3.27	1.122
0.01209	3.33	1.096
0.01109	3.33	1.078
0.01009	3.31	1.059
0.00909	3.27	1.047
0.00809	3.13	1.029
0.00709	3.06	1.023
0.00609	3.06	1.029
0.00509	3.00	1.000
0.00409	2.93	0.971
0.00309	2.86	0.917
0.00209	2.73	0.871
0.00159	2.66	0.866

*) Based on calculated f

BIBLIOGRAPHIC DATA SHEET	1. Report No. FFA R 127	2.	3. Recipient's Accession No.
4. Title and Subtitle Flow disturbances associated with Preston tubes in turbulent boundary layers			5. Report Date 6.
7. Author(s) Arild Bertelrud			8. Performing Organization Rept. No.
9. Performing Organization Name and Address The Aeronautical Research Institute of Sweden (FFA), Box 11021, S-161 11 BROMMA, Sweden			10. Project/Task/Work Unit No. 11. Contract/Grant No.
12. Sponsoring Organization Name and Address Defence Materiel Administration (of Sweden), Air Materiel Department			13. Type of Report & Period Covered 14.
15. Supplementary Notes			
16. Abstracts			
17. Key Words and Document Analysis. 17a. Descriptors 17b. Identifiers/Open-Ended Terms 17c. COSATI Field/Group			
18. Availability Statement No restriction on distribution. Available from National Technical Information Service, Springfield, VA. 22161 USA or issuing Act.		19. Security Class (This Report) UNCLASSIFIED 20. Security Class (This Page UNCLASSIFIED	21. No. of Pages 22. Price